Aalto University
School of Chemical
Engineering

Saana Lipasti

PREPARATION OF COBALT PARTICLES IN AQUEOUS MEDIUM AND DISPERSION STABILIZATION

Master´s Programme in Chemical, Biochemical and Materials Engineering
Major in Chemistry

Master's thesis for the degree of Master of Science in Technology submitted for inspection, Espoo, 28th July 2022.

Supervisor Prof. Tanja Kallio

Advisor D. Sc. (Tech) Olli Sorsa

Aalto University
School of Chemical Engineering

Aalto University, P.O. BOX 11000, 00076 AALTO
www.aalto.fi
Abstract of master's thesis

Author Saana Lipasti

Title of thesis Preparation of Cobalt Particles in Aqueous Medium and Dispersion Stabilization

Department Department of Chemistry and Materials Science

Professorship Electrochemical energy conversion and storage

Thesis supervisor Prof. Tanja Kallio

Thesis advisor(s) D. Sc. (Tech) Olli Sorsa

Collaborative partner Freeport Cobalt Oy

Date 28.07.2022 **Number of pages** 75 **Language** English

Abstract

Cobalt particles and powders are used widely across various industries and are especially important for the hard metal industry. The hard metal industry uses metallic cobalt as a binder in the production of tungsten carbide (WC). In the production, a powder spreads easily through the air, making the process difficult to control. Moreover, metallic cobalt is prone to reacting with air to form undesirable, even unusable cobalt oxide. In order to improve the handling and usage of cobalt and prevent oxidization, a novel product needs to be developed. This product concept includes preparation of fine powder (particles) by precipitation in an aqueous solution as well as dispersion of the prepared particles in an aqueous carrier fluid. This work studied precipitation experimentally and discusses dispersion stabilization based on the literature.

The first hypothesis was that the reduction of cobalt and preparation of particles are possible in water at mild temperatures with similar reagents proven to work in organic solutions. The cobalt source, reductant and surfactant were cobalt sulfate, hydrazine, and sodium citrate, respectively. The hypothesis was confirmed as pure metallic cobalt particles were produced in a series of experiments in alkaline aqueous solutions under nitrogen atmosphere. The second hypothesis was that the reaction, especially the particle size, can be controlled with the use of $AgNO_3$ as a nucleation agent. This could be partially confirmed but the series of three experiments can be considered only as limited evidence. The average sizes of the particles were in relation to the $AgNO_3$ concentrations. However, the growth of the particles was dendritic, so the size distribution was wide, and the reduction reaction was not better controlled compared to the first experiment series. Overall, more research is needed in order to use this chemical procedure in particle preparation for stable dispersion. Nevertheless, preparing highly pure cobalt particles is possible in water with a facile and fast technique.

Keywords cobalt, hydrazine, reduction, aqueous, particles, powder, dispersion

Aalto-yliopisto
Kemian tekniikan korkeakoulu

Aalto-yliopisto, PL 11000, 00076 AALTO
www.aalto.fi
Diplomityön tiivistelmä

Tekijä Saana Lipasti

Työn nimi Kobolttipartikkeleiden valmistus vedessä ja dispersion stabiloiminen

Laitos Kemian ja materiaalitieteen laitos

Professuuri Sähkökemiallinen energian muuntaminen ja varastointi

Työn valvoja Prof. Tanja Kallio

Työn ohjaaja(t) TkT Olli Sorsa

Yhteistyötaho Freeport Cobalt Oy

Päivämäärä 28.07.2022 **Sivumäärä** 75 **Kieli** englanti

Tiivistelmä

Kobolttipartikkeleita ja -jauheita käytetään laajasti eri teollisuudenaloilla ja ne ovat erityisen tärkeitä kovametalliteollisuudelle. Kovametalliteollisuus käyttää metallista kobolttia sidosaineena volframikarbidin (WC) tuotannossa. Jauhemaisena koboltti leviää herkästi tehden tuotantoprosessista vaikeasti hallittavan. Lisäksi metallinen koboltti on altis reagoimaan ilman hapen kanssa kobolttioksidiksi, jota on vaikea enää hyödyntää. Uudenlainen kobolttituote tarvitaan käsittelyn helpottamiseksi ja hapettumisen välttämiseksi. Tällainen tuotekonsepti sisältää hienon kobolttijauheen (partikkelien) valmistamisen sakkaamalla vesiliuoksesta sekä valmistettujen partikkelien dispergoinnin vesifaasiin. Tässä työssä tutkitaan sakkaamista kokeellisesti ja dispersion stabilointia teoreettisesti kirjallisuuden pohjalta.

Ensimmäinen hypoteesi oli, että koboltin pelkistys ja partikkelien valmistus ovat mahdollisia vedessä matalassa lämpötilassa reagensseilla, joiden on todettu toimivan orgaanisissa liuoksissa. Kobolttilähtöaine, pelkistin ja surfaktantti olivat kobolttisulfaatti, $CoSO_4$, hydratsiini, N_2H_4 ja natriumsitraatti, $Na_3C_6H_5O_7$, tässä järjestyksessä. Tämä hypoteesi osoittautui oikeaksi, kun puhtaita metallisia kobolttipartikkeleita onnistuttiin valmistamaan koesarjassa emäksisissä vesiliuoksissa typpi-ilmakehässä. Toisen hypoteesin mukaan reaktiota, ja erityisesti partikkelikokoa, voidaan kontrolloida käyttämällä hopeanitraattia ($AgNO_3$) ydintymisaineena. Tämä hypoteesi pystyttiin osittain vahvistamaan, mutta kolmen kokeen sarjaa voidaan pitää vain suuntaa antavana. Keskimääräinen partikkelikoko noudatti hopeanitraattipitoisuutta. Partikkelien kasvu oli kuitenkin haaroittunutta, mikä teki kokojakaumasta leveän, eikä pelkistysreaktio ollut paremmin hallittavissa verrattuna ensimmäiseen koesarjaan. Kaiken kaikkiaan enemmän tutkimusta tarvitaan, jotta tätä menetelmää voitaisiin käyttää partikkelien valmistamiseen stabiilia dispersiota varten. Joka tapauksessa puhtaitten kobolttipartikkelien valmistaminen vedessä osoittautui mahdolliseksi yksinkertaisella ja nopealla menetelmällä.

Avainsanat koboltti, hydratsiini, pelkistys, vesiliuos, partikkelit, jauhe, dispersio

Preface

I want to thank all the people who have helped and supported me as I have struggled with the thesis. People can be very kind-hearted and patient, as has been the case with Prof. Tanja Kallio and PhD Olli Sorsa. Olli has helped me with everything related to experiments and given indispensable feedback on the thesis. The thesis done in collaboration with Freeport Cobalt Oy. Other people who deserve to be mentioned are Freeport representatives Samuli Räsänen, Janne Marjelund, Kai Pulkkinen and Juha Järvi, as well as my study buddy Emmi Sveholm, Sanna Tervala and my study buddies from Klubitalo, Antti Kurkinen (general comments), Kenneth Pennington (language and structure), Anita Pirhonen (practicalities), (Syed M.) Farhan Ali (TEM imaging), and Eero Haimi (SEM sample preparation). Finally, I thank my love Heikki Niemi for being there for me, always.

Helsinki, 28.7.2022
Saana Lipasti

Table of Contents

1 Introduction

In a modern society, tough materials are used in cutting tools and machines as well as in components and coatings. These materials experience high friction, wear and temperature. In such conditions, hard metals are some of the most commonly used materials. Hard metals, also known as cemented carbides, contain cobalt (Co) as a binder between the carbide grains. Conventionally, cobalt is utilized as a powder in the production process of hard metals. However, as a powder, cobalt spreads easily through the air, making the process difficult to control. Moreover, metallic cobalt is prone to reacting with air to form undesirable, even unusable cobalt oxide. In order to improve the handling and usage of cobalt and prevent oxidization, a novel product needs to be developed.

One potential strategy for solving these handling and oxidation problems is to evenly disperse cobalt powder or finer particles into organic carrier fluid. However, this approach is currently limited by several challenges. The main issue with this strategy is that large quantities of organic liquids are needed for both precipitating cobalt particles, e.g., [1, 2, 3], and preparing a stable dispersion of the particles. Moreover, organic liquids are often hazardous for the environment, and require expensive logistics and handling processes. Although earlier research has successfully synthesized and dispersed nano-sized cobalt particles using organic liquids, little work has yet attempted to do this with larger particles using an aqueous medium. Especially, preparation techniques of cobalt particles using organic solutions, such as the polyol process, are well-known and utilized. At the same time, precipitating pure, metallic cobalt particles from aqueous solution has been studied surprisingly poorly.

The aim of this thesis is to identify key reaction parameters and methods for producing an aqueous cobalt dispersion. To accomplish this aim, a procedure will be

experimentally developed for synthesizing pure cobalt particles from an aqueous solution. This is done by precipitation without external current. The main focus is finding which reaction parameters have the most significant effect on the morphology, size distribution, and chemical composition of the particles. A secondary goal is to identify the most suitable chemical procedure to prepare particles which could be used to create a stable, homogeneous dispersion in an aqueous medium. Producing a stable, aqueous cobalt dispersion is scrutinized from a theoretical point of view.

The thesis is structured as follows. Chapter 2 provides background information on both fine and coarse cobalt particles. More precisely, it describes the most essential properties, production methods and applications of cobalt particles. Chapter 3 presents the main properties of and methods for producing a stable dispersion. In Chapter 4, the characterization methods used in the study are described, focusing mainly on their working principles. Chapter 5, Methodology, consists of two parts. Section 5.1 explains the procedure and reaction parameters for synthesizing particles from aqueous solution. Section 5.2 provides the methods for characterizing synthesized particles based on the methods introduced in the previous chapter. Chapter 6 presents and compares the characterization results for the experiments. Finally, Chapter 7 summarizes and discusses the most important findings as well as shortcomings of the study and makes proposals for future research.

2 Cobalt Particles and Powders

2.1 Properties and Applications

Cobalt (Co) has a unique combination of properties. It has a high melting point of 1493 ˚C and a high strength even at elevated temperatures. All properties of cobalt derive from its electron configuration [Ar] $4s^2$ 3 d^7. This structure enables multivalency (Co(+II) and Co(+III)), ferromagnetism with a good thermostability, creep resistant toughness, and multiple crystal structures (HCP, FCC, and epsilon). Magnetic and electronic properties of cobalt are dependent on the crystal structure.

The combination of properties and abundancy of cobalt in the earth make it a versatile element, which has a large number of applications. Cobalt has many well-known alloys and compounds. Hardness and toughness of cobalt enable the existence of many thermostable, corrosion and wear-resistant superalloys, and hard-facing alloys, e.g., one of the oldest commercial cobalt-based superalloy, stellite. The ferromagnetic properties of cobalt are utilized in medical applications, magnetic recording media, sensors, magnets, and ferrofluids. One example of ferromagnetic materials is the first electromagnet in history, aluminum-nickel-cobalt (AlNiCo). There are also plenty of cobalt compounds that are used as antimicrobial agents, catalysts for petroleum and chemical industries (e.g., in the Fischer-Tropsch process), as lithium-ion battery cathodes ($LiCoO_2$), as well as pigments and dyes. One important application of cobalt is the hard metals. Much of cobalt is utilized in forms of particles and powders of different coarseness. The powder metallurgy is an important industry which produces cobalt powders for the production of permanent magnets, superalloys, hard-facing alloys, tool and die steels and hard metals.

Hard metals are durable composite materials that comprise two parts: the hard phase, and the metal component. The hard phase, which is most commonly tungsten carbide

(WC), is hard but brittle. However, brittleness can be overcome by utilizing the metal component as a binder between the carbide grains. This leads to excellent hardness, wear resistance, and compressive strength. The crucial metal component, most commonly cobalt, is melted from powder and mixed with solid carbide grains.

2.2 Production Methods

Methods for Co particle production can be divided into two groups: top-down and bottom-up approaches. In top-down approaches, Co particles are prepared by physical processing, e.g., mechanically grinding grains or larger chunks of cobalt into smaller pieces. On the contrary, bottom-up approaches are based on chemical reactions. A framework for different production methods is presented in Figure 1. Top-down techniques include lithography, repeated quenching, milling, and attrition. [4] However, particles produced utilizing these techniques generally have a broad size distribution, inconsistent morphology, and impurities. In order to avoid these problems and to gain other advantages discussed in Chapter 1 and Section 2.2, this work focuses on the bottom-up approach, more specifically precipitation from solution.

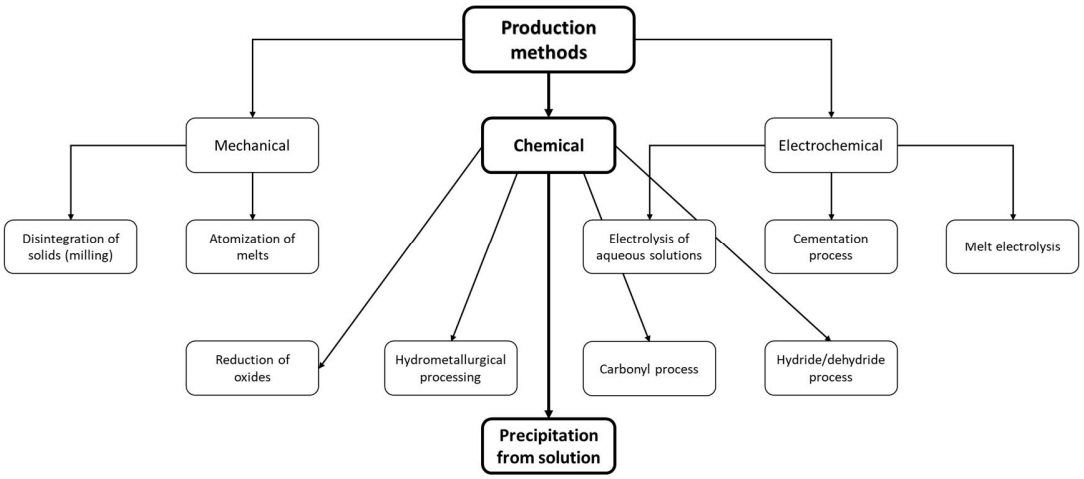

Figure 1. Classification of Co particle production methods based on a table presented in Handbook of Non-Ferrous Metal Powders [5]. This classification does not include the gas phase precipitation or spray granulation methods.

Bottom-up approaches are divided into two categories depending on whether chemical reactions are mainly limited by kinetics or thermodynamics. The kinetic method consists of techniques in which the concentration of precursors and amount of space are limited, leading to steric hindrance. Examples of techniques which limit space are aerosol and micelle synthesis. In micelle synthesis, a microemulsion is created by capping growing particles with a surfactant, thus separating them from the medium. The process of the thermodynamic method is comprised of three steps. The steps are generation of a saturated medium (liquid, gas, or solid phase), nucleation, and subsequent growth. Controlling these steps can be utilized to control the whole reaction and end product. The second experiment series of this work, called Phase2, studies whether the cobalt reduction reaction can be controlled better with the use of silver nitrate.

Metal and composite particles have requirements concerning the size, composition, crystal structure and agglomeration depending on the final application. Co particles are

produced in several sizes and morphologies. The tiniest particles are a few nanometers in size, from quantum dots to nanocrystals. Larger particles are hundreds of nm's, i.e., submicron, or even a few µm. Even larger particles usually are referred to as powder. Typically, particles with a narrow size distribution are desired. For example, particles with a wide size distribution cannot be effectively dispersed for long periods of time. Morphology of Co particles has a large variety. Possible shapes include solid and hollow spheres, wires, rods, cubes, and platelets to mention a few. Furthermore, combined with variety of crystal structures all shapes imaginable are possible. In the literature, unusual morphologies of Co crystals and particle formations have been described: flowers [6, 7], leaves [8, 9], ear of rice [10], snowflakes [11], and so many others. The variety of morphologies relates to at least two factors. Firstly, the slow nucleation stage compared to the faster growth stage favors dendritic formations. Secondly, primal particles have a high tendency to agglomerate and form larger units if they are not encapsulated with a protecting surfactant. Agglomeration is a serious problem when the obtained particles are meant for production of a stable dispersion or colloid. Keeping the goal of a stable dispersion for hard metal industry in mind, this work focuses on producing metallic Co particles of submicron or smaller in size, spherical in shape and covered in a protective layer of citrate to hinder agglomeration and oxidation. The stable dispersion is discussed in detail in the following chapter.

Cobalt is produced mainly from the following minerals: sulphides, arsenides, oxides, and hydroxides. [12] Co powders with a grain size of one micron or smaller are conventionally produced by pyrolysis of a cobalt salt, followed by milling down when needed. [12] This is the main route for manufacturing products for the hard metal industry. In case of nano-sized powders, or particles, a well-known production route is the polyol process where dissolved cobalt is precipitated from an organic solution. The organic solvent is a mixture of ethylene-glycol and diethylene-glycol. The polyol process enables production of spherical, non-agglomerated and pure cobalt particles.

[12] Table 1 presents results of a study [13] that compared impurity levels in powders prepared by solid-gas reduction and polyol process. In the study, two types of cobalt powders were produced from the same cobalt hydroxide. The key finding was that precipitation from a solution can produce a remarkably purer product. Especially, much less calcium and sodium can be found in cobalt reduced via the polyol process. This thesis aims for a cobalt product of high purity, which is one of the reasons to use precipitation from a solution as the approach.

Table 1. Main impurities in cobalt powders produced from cobalt hydroxide by solid-gas reduction and polyol process in [13]. Reported by impurity/cobalt ratio in ppm by weight.

Impurity element	Amount in cobalt hydroxide precursor (ppm)	Amount in cobalt powder produced using solid-gas reduction (ppm)	Amount in cobalt powder produced using polyol process (ppm)
Ca	150	150	< 5
Fe	80	80	20
Ni	250	250	250
Si	150	150	130
Cl	2000	500	60
S	150	150	< 50
Na	250	250	< 10

The polyol process is commonly used both in lab- and industrial scale. Using the polyol process, cobalt particles can be obtained with a narrow size distribution anywhere from nano- to micrometers by varying the reaction parameters, such as temperature, or introducing foreign nuclei to the reaction. Similar results could potentially be achieved in aqueous processes. More research is needed in this topic. The polyol process and producing cobalt using water-based solutions are discussed in the following section.

2.3 Precipitation from Solution

In this work, the cobalt particles are prepared by precipitation from a solution, more precisely from water. As discussed before, precipitation from solution can happen from organic liquids (organometallic and polyol processes) or water. Precipitation is an

inorganic reaction and synthesis method where ions dissolved in a solvent react to form a solid compound. The reaction takes place after the addition of a reducing or oxidizing agent. The precipitation of cobalt requires the solution to be supersaturated. This means the new compound needs to be insoluble after reaching a certain concentration, which depends on environmental factors, such as temperature. For metals, precipitation is a reduction reaction as they have dissolved into the solvent as positive cations. Therefore, methods of precipitation from solution are sometimes called liquid-phase reduction. Producing metallic cobalt directly from a solution without forcing the reaction by an electric current can be a very facile and economical method. Figure 2 shows the simplicity of an industrial pilot scale polyol process [13] as an example.

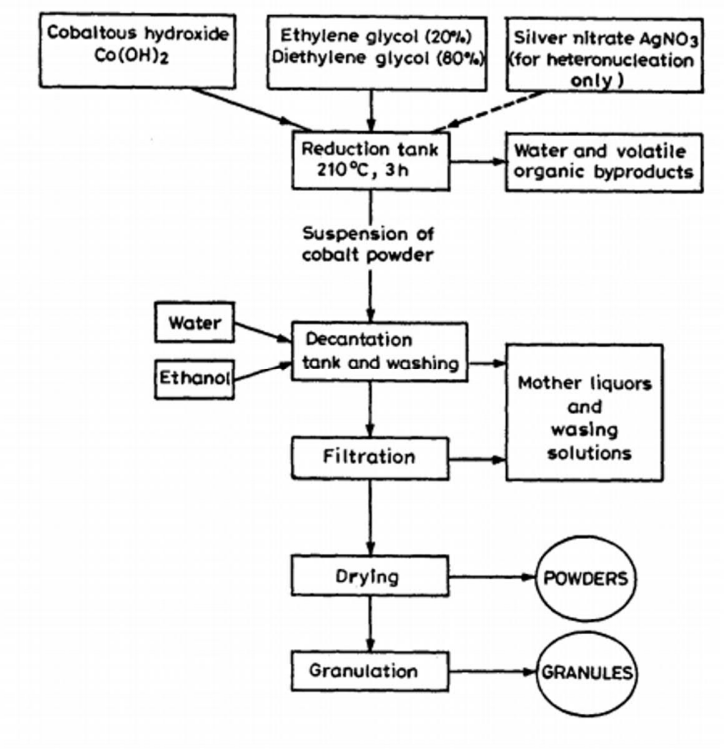

Figure 2. Process flow diagram of a polyol process as presented in [12], based on the work of Pastor et al. [13].

The properties of cobalt discussed in the beginning of the chapter affect the morphology and crystal structure of cobalt particles. The electron structure of cobalt causes a problem in case of metallic Co particles: individual particles tend to form clusters as they attract each other due to their magnetic nature. This is a larger issue for pure metallic cobalt particles as they are ferromagnetic to a greater extent than, for example, cobalt oxides. In addition to clusterization, the magnetism affects the growth process of cobalt particles by aligning cobalt that is getting reduced and deposited on the surface of already formed particles in a certain way. This produces larger and elongated particles, which might be undesirable. This kind of growth is more prominent in diffusion-controlled reactions and particles larger than nanometer scale. Fortunately, problems relating to magnetism can mostly be avoided by keeping particles from becoming magnetized. In this work, this was the reason the magnetic mixing system was changed to a mechanical one, even though the mechanical mixing system needed to be built from scratch.

As mentioned earlier, particle formation generally has three steps: supersaturation, nucleation, and growth. However, the nucleation step of a reagent of interest can be substituted by seeding or adding small amounts of an easily reduced and precipitated reagent. For example, the nucleation of cobalt could be bypassed using cobalt crystals (seeds) or dissolving salt of a noble metal, such as silver nitrate. After nucleation, colloidal particles grow either by molecular addition or agglomeration, e.g., Ostwald ripening. The famous LaMer model is used for formation and growth of monodispersed colloidal particles in homogeneous solutions. The LaMer mechanism was proposed by LaMer and Dinegar in 1950 [14] and is widely accepted, although more complex models are needed for heterogeneous solutions and other deviations from the presumptions of the model [15]. A modified presentation of the LaMer model is shown in Figure 3. During the prenucleation period, the concentration of the dissolved metal atoms increases and the solution becomes supersaturated. The second stage begins

when the concentration reaches the minimum nucleation concentration. The spontaneous self-nucleation occurs more and more frequently as the metal ion concentration continues to increase until a maximum concentration, critical limiting supersaturation is achieved. From there the concentration starts to decrease. As the concentration level meets the minimum nucleation concentration again, the nucleation ceases and the diffusive growth begins on the surface of the nuclei. The particles continue to grow as long as the concentration of dissolved metal atoms/ions stays over the saturation concentration.

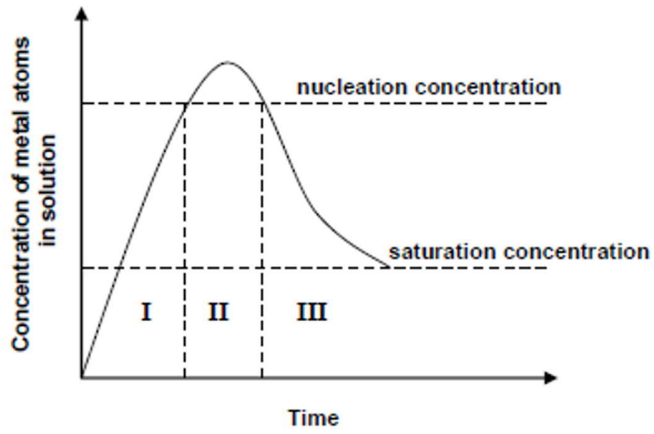

Figure 3. LaMer mechanism for monodispersed systems by controlled homogenous nucleation as redrawn in [16] based on visual presentation by Viau et al. 1996 [17]. The stages are I prenucleation period, II nucleation step, and III growth step.

Fievet et al. 1989, [18], suggested that reduction and precipitation of metals from liquid media is the only way to obtain metal particles of similar size and shape. Additionally, clear separation of nucleation and growth stages is necessary. This is acquired with seeding, by adding either crystals of the same metal or a salt of easily reduced metal. Moreover, agglomeration of the particles during their growth should be avoided, e.g., by using surfactants. The growth step has to be controlled as too fast growth consumes Co ions and their diffusion to the surface of particles becomes the

limiting factor. This leads to dendritic growth instead of rounded particles. [19] Figure 4 shows how poly-nuclear growth can lead to narrower size distribution.

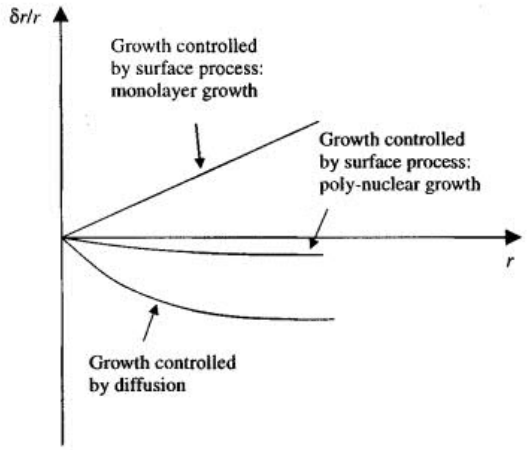

Figure 4. The relative difference in radius among nanoparticles of different growth mechanisms as a function of particle radius as presented in [4].

In this work, silver (Ag) is used as foreign nuclei to initiate poly-nuclear growth. Ag gets reduced much more easily in water compared to Co, as can be seen in the electrochemical series. If the use of Ag must be avoided, metallic Co particles could be used as a seed instead. As in the case with any seed, size of the final seed-Co particles depends on the amount of seed particles (which depends on the initial concentration of seed-forming ions, e.g., Ag^+ ions). Similarly, increasing the initial concentration of Co does not necessary increase the size of primary particles at a given number of a certain type of seed particles. At first, increasing the Co ion concentration increases the average particle size. The growth of the particle size is approximately linearly dependent on the initial Co concentration at a certain very narrow concentration range. However, using even higher initial Co concentrations leads to formation of new Co nuclei and decrease in the average particle size. If a larger particle size of narrow size distribution is the desired outcome, seedling the reaction solution with either Ag or Co can be beneficial. Using seeds or nucleation agents is a conventionally used

solution in similar cases. For example, these polyol process experiments with nickel and cobalt successfully utilized silver as a nucleation agent [18]. The relative amount of the nucleation reagent to the initial concentration of Co is also important acquiring as pure Co particles as possible. In the end, Ag is considered as an impurity in the final product, despite being useful in the production process.

In addition to separating the nucleation from the growth step, a reaction can be controlled by regulating the temperature and acidity level, as well as varying the initial concentrations of each reagent and the reagent order, and utilizing a surfactant. A total or partial control can be achieved over the mean particle size and size distribution, the growth way and final shape of the particles, conversion degree, reaction speed, agglomeration, and clustering degree. Many of these aspects are crucial to achieving a viable method for producing a novel Co product, whether the final product be a dry powder or particles dispersed in water. The temperature affects the whole reaction, its speed and effectively the conversion rate as well. While conversion rate was not under the scope of this study, suggestions for conversion rate studies are included in the final chapter. Naturally, reagent concentrations and their relations have a significant role in the experiments. There has to be large quantities of N_2H_4 compared to Co, as it is not only consumed by the reduction reaction but also gets vaporized in the reaction temperatures of around 50 ˚C. Proper mechanical mixing is required to avoid significant concentration gradients. This is especially true when introducing N_2H_4 to the reaction solution. Mechanical mixing is important as a magnetic stirrer would result in magnetic forces that guide the growth of Co particles in elongated forms. Furthermore, as growing particles are being gathered to the surface of a magnet, notable concentration gradients are formed in spite of vigorous mixing.

Surfactants can have several roles in the reaction and are called by different names accordingly. The term ’surfactant’ generally refers to a molecule that reacts on or

attaches weakly to the surface of a particle and changes its reactivity and, therefore, many properties. A capping agent is a surfactant that affects the growth of the particle, normally hindering and finally stopping it. Especially, polymers and other large molecules hinder the diffusion of Co ions to the surface of the particles making the growth step of the reaction a diffusion controlled. This affects the whole reaction rate, the size of the final (primal) particles and the degree of clusterization and agglomeration. A protective agent works in a similar way as capping agents but also protects particles from oxidation. A dispersant or dispersing agent keeps the primal particles separate and spreads them to a larger area. Sometimes, this means that particles end up floating on the surface of the carrier liquid or sink to the bottom of the container, sometimes, that particles remain evenly dispersed in the whole body of the carrier liquid as the dispersing agent makes them to repel each other strongly and makes their effective density close enough to the density of the carrier liquid. In the case of the latter, the concentration of the particles is the same in every part of the carrier liquid, which is desirable to a Co product for hard metal industry. Sometimes, a surfactant participates both in the nucleation and growth steps as in the case of citrate ion: citrate forms coordination complexes with Co ions both in aqueous and organic media acting as a catalyst but, additionally, adheres on the surface of the final particles protecting them from clusterization, agglomeration, and oxidation. Moreover, citrate improves the reducing power of hydrazine and the overall reaction speed [9]. Citrate and other capping agents are utilized both with organic and aqueous solutions. However, many organic solvents themselves have provide similar steric and diffusion-inducing effects, and, therefore, incorporation of capping agents is not necessarily required in those reactions. In this work, citrate participates in the reaction as it coordinates strongly with metallic cobalt, water molecules and all ions that are present. As the reaction mechanism is not fully understood, citrate may have a major or minor role in the reaction.

NaOH is often used to regulate the pH of the solution. At high pH levels, hydrazine reacts as presented in Equation (2). In comparison, Equation (1) shows corresponding reaction in acidic conditions, which is more typical to cobalt reduction in organic media. The acidity level, or pH level, of solution is important for the reaction as it only takes place over certain level. In the case of aqueous solutions, the reduction reaction stops completely at around pH 9-11, but the pH level is advised to be maintained at 13-14 in order to achieve a reasonable reaction rate. A study [19] with a relatively similar chemical reaction to this work determined the minimum pH levels to be 12.1 on a metal surface and 12.6 in the bulk solution. The oxidation reaction of N_2H_4 consumes OH^- ions and, therefore, its reducing power is remarkably higher at pH values 13-14. [9] In this work the pH level is set initially to 14, but since OH^- ions are consumed the main and side reactions, the pH level decreases over time. The decline in pH level seems to be one the main reasons the reaction ceases before any other reagent is totally consumed. In fact, OH^- ions seem to coordinate with other ions, including cobalt and partially electrically charged molecules similarly to $C_6H_5O_7^{3-}$ ions. In most reactions, the pH level is adjusted by NaOH before adding N_2H_4. This is justified by the fact that the addition of N_2H_4 does not considerably affect the pH level.

$$N_2H_5^+ \leftrightharpoons N_2 + 5\ H^+ + 4\ e^- \quad (1)$$

($E^0 = 0.23$ V)

$$N_2H_4 + 4\ OH^- \leftrightharpoons N_2 + 4\ H_2O + 4\ e^- \quad (2)$$

($E^0 = 1.16$ V)

3 Dispersion Stabilization

As briefly discussed in the previous chapter, metallic Co particles of narrow size distribution could be used for a novel product for hard metal industry if they could be stably dispersed in a liquid medium. This kind of new product might be superior to dry powder products for its finer structure, better protection towards oxidation, and advantage of not spreading in air.

3.1 Definitions of Dispersion Stability

The dispersion stability of metallic particles in a liquid medium can be defined in three ways. First, the dispersion stability can simply mean that the particles will not get oxidized in a relatively long period of time. Co is prone to oxidation as a non-noble metal (Standard Reduction Potential −0.28 V). This means that, in order to keep the Co particles metallic, the particles need to be protected by surfactants after precipitation under N_2 atmosphere. Second, the macroscopic stability requires the particles remain evenly dispersed in the whole medium. This is especially hard across the vertical dimension against the gravity. The last way a dispersion can be stable is the microscopic or colloidal stability. A microscopically stable dispersion has particles that keep their own identity. The microscopic stability is almost always the basis for the macroscopic stability in a system in which the densities of the dispersed phase and dispersing medium differ notably. This work addresses all three kinds of stability but this chapter focuses on means to achieve microscopic and macroscopic stability.

Particles can lose their identity either by agglomeration or sintering, e.g., Ostwald ripening. Agglomeration happens when particles form clusters as they become loosely attached to each other. This process can lead to aggregates if particles form chemical bonds. In this work, the term agglomeration (forming of agglomerates) refers to both clusterization (clusters) and aggregation (aggregates), but the nomenclature greatly

varies in different sources depending on the field and application [20]. Aggregates can be broken down into smaller units, but primary particles are almost impossible to restore. As aggregates are divided into smaller nanostructures their bonds become increasingly stronger [4]. In addition to agglomeration, particles can lose their identity by sintering. Sintering means that the individual structures, such as single domain particles or larger entities, merge together. Ostwald ripening is a mechanism of sintering where smaller particles dissolve and the matter deposits onto the surface of larger particles. Microscopic instability is caused by the particles' tendency to minimize the surface energy.

This chapter mainly focuses on stabilization against aggregation, i.e., microscopic stabilization. Microscopic stability is a requirement for macroscopic stability in most cases, as growing larger aggregates create a gravitational gradient within the solution. In simple terms, if particles form large enough agglomerates, they will settle to the bottom of the container. Microscopic stability is affected by the surface energy of the particles. When particles increase in size, the volume increases faster than surface area. Therefore, a smaller percentage of atoms in a particle are surface atoms. Only surface atoms create surface tension, which causes the microscopic instability, as particles aim to minimize this free energy. Figure 5 shows the general trend in the relative amount of surface atoms in a spherical, relaxed particle. While the data is for palladium (Pd) particles, it is reasonable to expect similar trend if it were for cobalt particles. However, there might be a difference in corresponding diameters, as Pd atoms are larger than Co atoms and their crystal structures may differ.

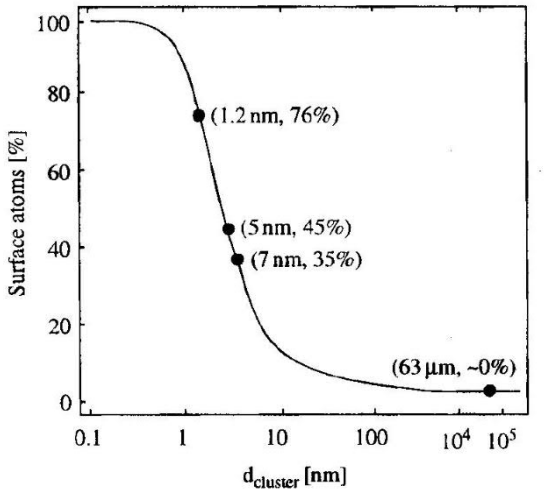

Figure 5. The percentages of surface atoms with respect to the total number of atoms in palladium clusters [particles] of different diameters. This modified illustration was presented in [4] and the data and original graph were presented in [21].

While larger particles have relatively less surface atoms, which contribute to interparticle attractive forces, they experience greater gravitational forces as Co is denser than common solvents. In conclusion, smaller (nano)particles are microscopically less stable, whereas larger particles are macroscopically less stable. These instability issues can be tackled with methods discussed in Section 3.3.

3.2 Properties of Stable Dispersion and Stabilization Methods

The forces that support the dispersion stability are entropy and osmotic pressure. The properties of a dispersion that support the dispersion stability are small effective density gradients, low ionic strength, repulsive forces created by particles (and attached surfactants) with like charges, homogeneity of particles in terms of size, form, chemical composition and structure, a low original molarity of Co and a small size of the precipitated and dispersed particles. The stability is weakened leading to density gradients or separation of phases (clusters, aggregation of particles, sedimentation, creaming) by the following forces: the gravitational force (large effective differences in density) and Van der Waals forces. Other factors which cause instability consist of

screening of counter ions (smaller effective charge), bridging caused by surfactants, time (thermodynamically unstable system), energy from outside the system (mechanical stirring), changes in temperature or magnetic field, and movements of the container of the dispersion (moving sideways or upwards, tilting and vibration).

The term colloid can refer to the whole system, in which case the term colloidal suspension is an unambiguous option. Sometimes, a colloid can be used to refer to the dispersed substance (e.g., in this case, the surfactant-covered cobalt particles). In this work the terms colloid, colloidal suspension and system are used interchangeably in accordance to IUPAC definition. In this chapter, the term 'particle' refers to the cobalt particle precipitated earlier and the surfactant(s) (the original citrate layer or whatever substance it has been changed to). Sometimes 'particle' is replaced with 'primary unit' in contrast to a loosely agglomerated group of particles, in which case the term used is a 'cluster'. Clusters can be part of macroscopically stable colloid. If strong chemical bonds are formed between primary particles directly or due to surfactant bridging, they form heavy aggregates that settle to the bottom immediately after stopping stirring or heavily shaking. The liquid medium in which the particles are suspended can be referred to as the continuous or aqueous phase.

Stable colloidal systems, i.e., stable dispersions, can be divided into three categories: emulsion, gel, and sol. These colloid types and corresponding terminology is presented in Table 2. The most relevant type for the hard metal industry is sol, which is discussed in detail in the next section. Emulsion is also of interest, as it enables larger particles to be dispersed, and allows use of organic solvents but in smaller amounts. A rule of thumb is that agglomerates or primary particles larger than 100 nm separate from the carrier fluid [22] but this does not apply to emulsion. However, using emulsion as a stabilization method for large cobalt particles in an aqueous liquid requires the use of

organic liquids in relatively high quantities. Therefore, this chapter focuses on the sol method.

Table 2. Types of colloids and terminology.

Colloid	1. Emulsion	2. Sol	3. Gel
Primary unit	Droplet	Solid particle	Solid particle
Agglomeration	Coalescence	Flocculation (Coagulation)	Flocculation
Aggregation	Formation of larger colloidal particles	Slurry	Polymerization
Separation of phases	Sedimentation, Creaming	Sedimentation	-
End result	Two liquid phases	Clay (or cake) + solution = slurry	Dense or solid-like liquid

3.3 Stabilization Mechanisms for Sols

The main sol stabilization mechanisms against agglomeration and aggregation are based on steric and electrostatic repulsion. These repulsive forces are created by utilizing surfactant attached on the surface of suspended particles. In addition to sols, this kind of surface modification can be used for emulsions, where surfactant is adsorbed onto a particle within a micelle, to improve solubility, for example. Sterically stabilized systems are thermodynamically stable, whereas colloidal systems utilizing electrostatic repulsion are considered kinetically stable, which means the stability deteriorates over time. [4] Nevertheless, either of the stabilization mechanisms may provide long-term stabilization, which is crucial for the purposes of the hard metal industry. The most effective approach is applying both techniques simultaneously. This can be achieved with the use of polyionic surfactants.

An electric charge spontaneously develops on the interface of any suspended solid particles and a polar or electrolyte carrier liquid. According to Cao [4], the occurrence of an electric charge can be attributed to the following phenomena:

(1) Preferential adsorption of ions
(2) Dissociation of surface charged species
(3) Isomorphic substitution of ions
(4) Accumulation or depletion of electrons at the surface
(5) Physical adsorption of charged species onto the surface

In this work, particles of metallic, neutrally charged, cobalt are suspended in a polar solvent, water. The particles are synthesized using negatively charged citrate ions that get physically adsorbed on the surface of cobalt particles. The electric charge of citrate ions induces a positive charge on the surface of cobalt particles. However, citrate molecules are small in size and possess a low electric charge compared to polymers and polyion surfactants, for instance. Therefore, citrate ions are neither enough to prevent microscopic nor macroscopic instability for a system consisting of water and cobalt particles that are larger than a couple of nanometers in diameter. Instead, another kind of surfactant is required in order to produce a stable cobalt-water dispersion.

3.3.1 Steric Stabilization

Through the steric stabilization method, we can arrive at a microscopically, and even macroscopically, stable dispersion. Owing to steric hindrance, the primary units do not meet and form larger units, i.e., agglomerates or clusters making them microscopically stable. For instance, metallic cobalt particles keep their identity and size as given upon the synthesis reaction described in the thesis, should the particles to be used for a dispersion. Effects on macroscopic stability are less straight-forward as steric

stabilization can both prevent and cause forming of concentration gradients through the system.

The steric stabilization method is especially important in case of nonaqueous (organic) dispersions. Nonaqueous liquids typically have a low dielectric constant, which makes electrostatic stabilization a less viable approach [22]. The steric stabilization not only prevents primary units reacting with each other but also inhibits unwanted reactions with other species in the dispersion systems. In our case, cobaltous primary units are kept from reacting with dissolved oxygen.

Sterically stabilized dispersions are thermodynamically stable. This makes dispersions stable for a long time. They are less vulnerable to energy brought from outside, e.g., due to temperature fluctuation or vibration during transit. Furthermore, particles are always redispersable [4]. Other benefit of steric stabilization is that it makes systems less sensitive to impurities or trace additives compared to the electrostatic method [22]. The approach is effective in dispersing high concentrations of particles [4, 22]. In our case, this enables preparation of dispersions with higher cobalt/water mass relations. Furthermore, if surfactants used for steric stabilization are introduced to the system already during synthesis of the particles to be dispersed, the growth of the particles becomes diffusion-controlled. This makes it easier to achieve spherical, mono-sized particles that are needed for a stable dispersion.

In sterically stabilized systems, particles are physically blocked from getting close to and interacting with each other. Instead, the chains of the polymer surfactant molecules anchored to the surfaces of the particles interact with each other in a repulsive way as particles approach each other. The interaction of surfactants creates a barrier potential by steric exclusion. Steric stabilization works through several phenomena of which the most notable are the volume restriction and osmotic effects [4, 23]. Firstly, when the dangling chains of polymer surfactants attached on different

sol particles collide, the chains experience compression. This results in volume restriction of those polymer molecules and reduction of their configurational entropy. This can be mathematically expressed by a free energy of entropic (or elastic) interaction G_{el}. Secondly, as the chains of polymer surfactant molecules overlap, the osmotic pressure is increased. The osmotic pressure increases with higher solubility of the chains in the chosen carrier fluid. The osmotic repulsion between two sols covered with a polymer surfactant is described by a free energy of mixing interaction G_{mix}. A total free energy of interaction of a sterically stabilized system can be estimated as

$$G_s = G_{el} + G_{mix}\,, \tag{3}$$

where G_s is the steric interaction free energy

G_{el} is the entropic interaction free energy

G_{mix} is the osmotic pressure interaction free energy

In addition to the repulsive forces described above, a polymer surfactant can provide means to distribute the particles in the carrier fluid in a more evenly manner. A well-chosen polymer surfactant aids larger (submicron) particles to partially 'dissolve' into the carrier fluid. This happens through solvation, hydration in case of water, as the polymer experiences swelling by interacting solvent molecules. The degree of this desirable effect is temperature and carrier fluid (solvent) dependent. This takes place by reducing the surface or interfacial tension [22]. The surfactant may also lower the density gap between the particles and carrier fluid. This inhibits sedimentation or creaming. Sedimentation occurs when primary units are not of nanoscale or are dense compared to the carrier fluid. On the other hand, creaming occurs when primary units are lighter than the carrier fluid. In our case, pure cobalt particles are denser than water, and therefore, the difference can be overcome by introducing organic polymer surfactants of low density.

As discussed earlier, a good surfactant is compatible with the carrier fluid in terms of (partial) solubility and density. Additionally, polymer surfactant should consist of lyophobic, i.e., solvent repulsive, and lyophilic, i.e., solvent attractive, chemical groups [22]. A lyophilic group is a long, stabilizing chain that gets solvated by the carrier fluid. Let us refer to this part of a polymer as block A. A lyophobic group adsorbs on the surface of a particle that we want to disperse. This group is typically insoluble into the carrier fluid but is attracted to the particles. Let us call this part of the surfactant an anchor chain B. A typical structure of a polymer surfactant is A-B, A-B-A block, or BA_n (i.e., grafted copolymer). These structures and their behavior on the particle surface are illustrated in Figure 6. [23] Polymer surfactants that irreversibly bind to a solid surface by one end only (A-B block) are categorized as anchored polymers. Anchored polymers experience less bridging but are hard, if not i.mpossible, to remove. This lack of removability is a remarkable downside for cobalt products in which the polymers are considered as impurities. Benefits of anchored polymers include their suitability for concentrated colloids, and the fact that the particles can be redispersed if needed later on. If polymer surfactants only adsorb weakly at random points along the polymer backbone, they are called adsorbing polymers. Adsorbing polymers are a great option when polymer layer needs to be removable. Their pitfalls include bridging and weaker stabilization in general.

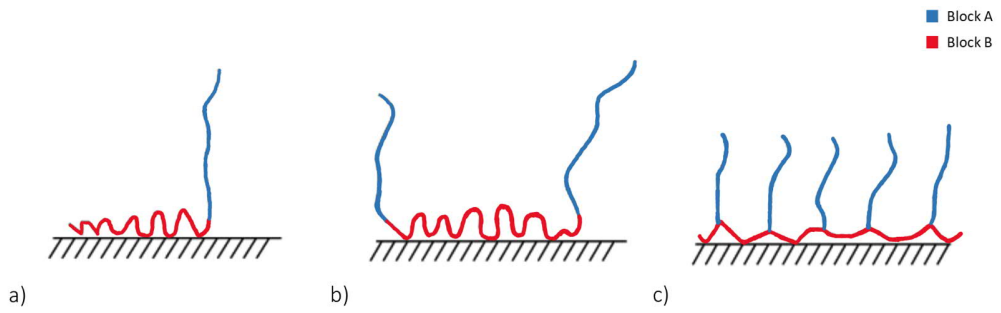

Figure 6. Typical interaction of polymer surfactants of different structure types with a solid surface: a) A-B block, b) A-B-A block, and c) $(AB)_n$ grafted copolymer. [23]

The major problems with steric stabilization are the following. First, the surfactant needs to be a larger molecule, such as a polymer, for any particle with a diameter larger than a few nanometers. This leads to a low core/surfactant ratio. Second, the particle-polymer unit size is always significantly larger than nanoscale, which leads to sedimentation as the effect of gravity is more impactful than that of entropy. This makes maintaining macroscopical stability a harder task to do. Third, dangling of A block chains of polymer surfactants can lead to bridging, especially common with A-B-A block polymers, or entanglement of the chains.

3.3.2 Electrostatic Stabilization

Electrostatic stabilization is a method that works especially well for stabilizing dilute aqueous sol dispersions. Electrostatic stabilization is based on overlapping of electric double layers around electrically charged particles [4]. As the double layers need to overlap for the repulsive force to emerge, the electric force does not affect particles out of the immediate proximity of a particle [4]. For this reason, the electrostatic method provides stability to the system on a microscopic scale. Therefore, electrostatic stabilization cannot be used to strive for even distribution of particles across a medium. Dispersions stabilized by electrostatic repulsion are kinetically stable. They can be very stable if the energy barrier created by the repulsive force is large. However, if agglomeration occurs, the system is not redispersable.

The theory of electric double layers is called DLVO after Boris Derjaguin, Lev Landau, Evert Verwey, and Theodoor Overbeek. A double layer is comprised of the Stern layer (compact double layer) and Gouy-Chapman layer (diffuse double layer). For a double layer to develop, an electric force needs to form between any electrically charged solid surface and species of opposite charge (counter ions) in an electrically conductive solution. Moreover, the surface of an originally neutral particle can induce a charge

due to polarization by ions in surrounding carrier fluid or by introduction of charged surfactants. In the latter case, the charge is more permanent in nature. Therefore, 'the charge of the particle' refers to the combined charge of the original (neutral or charged) particle and all attached surfactant molecules in the thesis.

Let us go over the structure of a typical double layer using this thesis's case as an example. We refer to Figure 7 and use the corresponding numbers. The following situation is after preparing and washing the cobalt particles. The surfaces of electrically conductive, metallic cobalt particles become positively charged due to polarization, as negatively charged citrate ions attach loosely onto them. Partially charged surface atoms/ions and negatively charged citrate ions form joint electron orbitals, but the bond is weak and therefore, I consider them as counter ions and not surfactants in this subsection. The Stern layer, (3), consists of the inner Helmholtz plane, (1), where adsorbed citrate ions screen the surface charge that they induced, and outer Helmholtz plane, (2), where positively charged ions (e.g., Na^+ and H^+) screen citrate ions. The Gouy-Chapman layer, (4), is the second part of the double layer, beside the Stern layer. The Gouy-Chapman layer contains totally solvated electrolyte species in decreasing concentrations until the concentrations equal the bulk phase concentrations. Outside the Gouy-Chapman layer remains the bulk phase, (5), which forms most of the suspension. The system behaves almost ideally if the concentrations of the dissolved and suspended species are low enough. In order to make a more evenly distributed and stable system, we should consider using a highly charged surfactant and make other modifications as well.

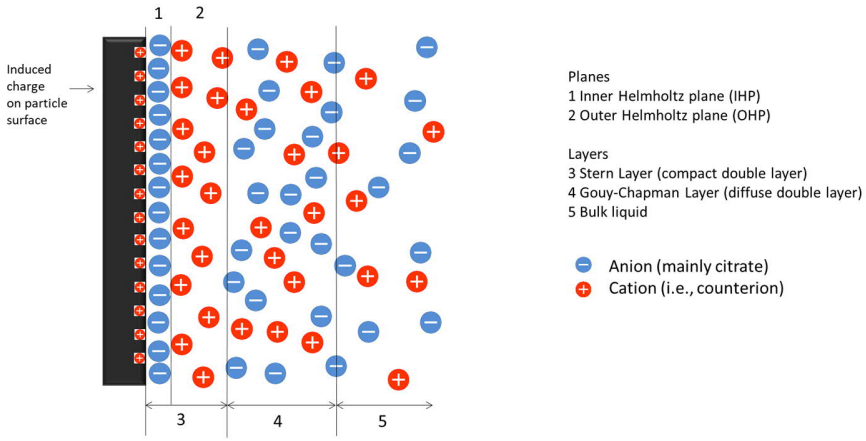

Figure 7. The structure of the electric double layer that forms in the particle-solution interface.

Theoretically, the repulsive force Φ_R between particles can be used to estimate the stability of a dispersion. The repulsive force can be estimated by using the DLVO theory as is shown below based on [4]. The electric potential E relates to the distance h from the surface of a particle as follows:

$$E \propto e^{-\kappa(h-H)} \tag{4}$$

where $1/\kappa$ is the Debye-Hückel screening length and describes the thickness of the double layer

$h \geq H$ and is the distance from the surface

H is the thickness of the Stern layer

$$\kappa = \sqrt{\frac{F^2 \Sigma_i C_i {Z_i}^2}{\varepsilon_r \varepsilon_0 R_g T}} \tag{5}$$

where F is Faraday's constant

C_i is the concentration of the counter ions of type i

Z_i is the valence of the counter ions of type i

ε_r is the relative permittivity or dielectric constant of the solvent (carrier fluid)

ε_0 is the permittivity of vacuum or the electric constant

R_g is the gas constant

T is the temperature

The electrostatic repulsion arises between two spherical particles when they approach each other, and their double layers overlap. The repulsive force Φ_R between two equally sized particles of radius r with a separation distance S can be estimated as:

$$\Phi_R = 2\pi\varepsilon_r\varepsilon_0 r E^2 e^{-\kappa S} \quad (6)$$

The DLVO theory and equations based on it (Eq. 4, 5, and 6) make several assumptions. A complete list of assumptions of the DLVO theory is given in [4]. The original DLVO theory assumes the following five premises. Firstly, there is an infinite flat solid surface, instead of randomly shaped particles with dangling, long surfactants on the surface. Secondly, the surface possesses a uniform charge density. Thirdly, the surface charge remains stable. Fourthly, the concentration profiles of charged species do not change. The latter two assumptions are required for the electric potential remain constant. Fifthly, no chemical reactions occur between the particles and solvent.

Although, no real system fulfills all the assumptions of the DLVO theory, it can be used to describe systems that satisfy the following less strict conditions [4]:

1) *The dispersion needs to be very dilute.*
2) *The only significant forces present are the van der Waals force and electrostatic potential. For the gravitational forces to be negligible, particles need to be small or of the same density as the rest of the solution. There should be no strong magnetic field, which can be problematic in case of metallic cobalt particles.*
3) *The geometry of the particles should be simple and regular, and the surface properties consistent all over the particles.*
4) *The double layer is purely diffusive in nature. The distribution profiles of ions in surrounding liquid are affected by electrostatic, entropic, and Brownian forces*.

These features are requirements for consistent surface charge density and distribution as well as electric potential in the surrounding medium. Therefore, evenly sized,

sphere-shaped particles with evenly distributed surfactants are the easiest to utilize for an electrostatically stabilized colloidal system. The DLVO theory should be used as guide for planning a dispersion system, but it cannot be used as a way to reliably calculate and predict how the system will work. Instead, a lot of experimental work needs to be done in order to acquire exact knowledge on a complicated system.

The electrostatic repulsion can be interpreted to be caused not only by interaction of the double layers but also osmotic flow [4]. The electric double layer consists of solution with higher concentrations of counter ions than the bulk solution. The concentration gradients are in equilibrium, which is disrupted when two particles come closer to one another. More solvent needs to flow between the particles to restore the equilibrium, pushing particles (and their double layers) further away from each other. Electric force is either a net attractive or repulsive force. The attractive, repulsive, and net forces are presented in Figure 8. The attractive van der Waals force is relative to the inverse of the distance between two particles with an exponent of 3-6. The repulsive force is inverse of the second power of the separation distance. [22] Therefore, two minima are present for the net electric force, as can be seen in Figure 8. The primary minimum represents the point where aggregates begin to form, and the secondary minimum correspondent to the point where flocculates (clusters) emerge [22]. The potential energy maximum is called the repulsive barrier, and it represents the energy required for a permanent agglomeration to take place [4]. The higher a potential energy maximum, the more stable the dispersion. Many factors affect the height of that peak, such as the charge of the surfactants. Those factors are covered later in this subsection.

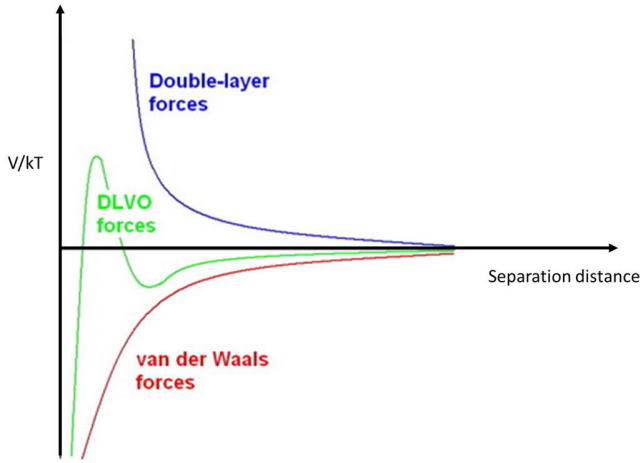

Figure 8. Forces according to the original DLVO theory. Figure modified from the one presented in [24].

In the case of polyionic surfactants, both electrostatic and steric stabilization mechanisms are utilized. The total potential energy in this is derived from the extended Derjaguin-Landau-Verwey-Overbeak (XDLVO). It is presented in Figure 9. In an ideal case, there is no definitive potential barrier to overcome. In practice, other reactions, e.g., collapse of double layers or bridging, occur as two particles are forced into each other's immediate proximity.

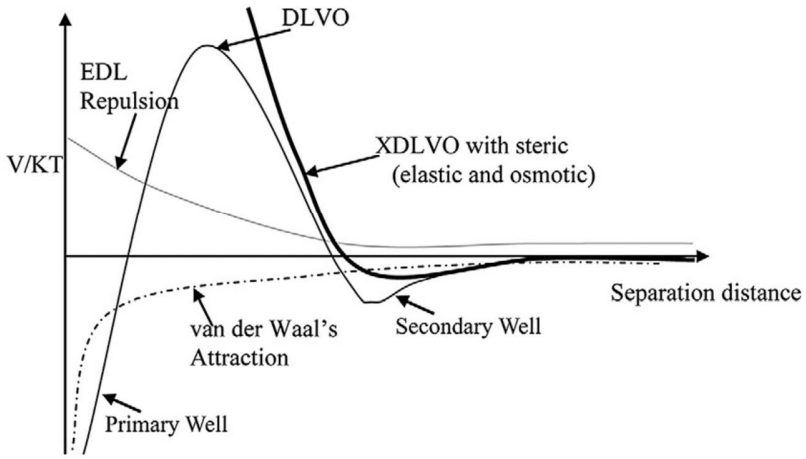

Figure 9. Forces according to the extended DLVO theory, XDLVO, as shown in [25].

The magnitude of the repulsion is related to the thickness of the double layer. The thickness can be represented by zetapotential in mV (e.g., [26]). The minimum thickness of 25 mV is required for a stable dispersion with no agglomeration [22]. Electrostatic stabilization requires a high dielectric constant of the solvent. This means that electrostatic stabilization is not applicable for the most common organic solvents, but water is a great choice as a carrier fluid. Dispersed particles need to be individual and separate, e.g., not dendritic or agglomerated, in order to acquire a constant surface charge density. Round particles are preferable for more uniform charge distribution [4].

To fill the requirement for the system as stated earlier, particle concentration needs to be low enough, unlike in the case of steric stabilization. This is required for preventing the charge distribution on a particle's surface to be influenced by other particles [4]. High particle concentration would also disturb formation of double layers. For the electric repulsion to be as effective as possible, the charge of a particle another particle 'sees', the effective charge, has to be as high as possible. Therefore, the shielding effect from the counter ions has to be mitigated. This can be achieved with a low total ionic concentration, low valence state of counter ions and larger size of counter ions [4, 26]. All these measures aim to lower the volume charge density of counter ions in solution surrounding a charged particle. Ideal surfactants are highly charged to create a larger repulsive force. For this reason, polyionic surfactants should be considered. With their large size, they also provide steric stabilization. It is crucial that the polymer surfactant is highly dissolvable in the solvent, so that it swells and unwinds. This is not affected only by the selection of surfactant and solvent pair but also by the temperature.

The agglomeration behavior of a surfactant-particle entities is dependent on its charge. A neutral surface charge minimizes the surface tension between solid and liquid phases

which can lead to flocculation or aggregation of particles. Also, when there is no electrical charge keeping particles from each other's immediate proximity, short-range attractive forces become significant (most notably magnetic attraction but also London forces). At this point, flocculants and aggregates settle to the bottom or float onto top due to gravity. How long this takes, depends on the density differences but also viscosity of the carrier fluid. In case of large aggregates, the determining variable is the friction between aggregates and the carrier fluid. On the hand, the main factor is the internal friction of the carrier fluid for tiny aggregates and single particles.

The situation differs for charged surfactant-particle entities. The electric repulsion is a significant force, which increases exponentially as the distance becomes shorter. However, counterions partially shield the charge but not the magnetic attractive force. According to the Schulze-Hardy law, counterions with a charge of a high absolute value make this process faster, as smaller number of ions shields the repulsive force in an effective manner. This makes a dispersion more stable when there are little or no high-charge ions. For instance, sulfate ions SO_4^{2-}, which are present in the solution when cobalt sulfate $CoSO_4$ is used as a precursor, hinder the useful repulsion between charged surfactant-cobalt particles more effectively than chloride Cl^- from $CoCl_2$ precursor. This means the selection of the cobalt precursor or washing the particles from effective counterions can have influence on the stability of a dispersion. The size of counterions has an effect on their ability to shield the surface charge of the surfactant or bare particles as it affects how close counter ions get to the particles. Similarly, the general shape and details of the surface structure affect the distance between a surface and counter ion. The shielding effect can be hindered, and therefore the magnitude of interparticle electrical repulsion maintained, by keeping the counter ions far enough. The physical properties of ligands or surfactants of importance include the shape, size, and flexibility. A polar ligand diminishes the surface tension between the ligand, i.e., particles, and the aqueous phase.

Aggregation can be limited thermodynamically or kinetically. If the dispersion is not thermodynamically stable, the preservation is statistically worse as the energy barrier is from time to time overcome and irreversible aggregation occurs. This is especially important for dispersion products that potentially experience vibration and temperature changes during transportation and storage.

Zeta potential can be used for determining the mean double layer thickness of particles. In practice, the thickness of a double layer predicts particles' tendency to agglomerate (and form clusters) and aggregate in addition to kinetic preventive measures. Zeta potential is almost linearly dependable on the pH level of the carrier fluid. Positive and negative zeta potential separate particles equally. The highest absolute zeta potential values are seen at very high and low pH levels as was observed in the experiments by Andrade et al. in 2012. The measurements were performed for iron oxide samples and are presented in Figure 10.

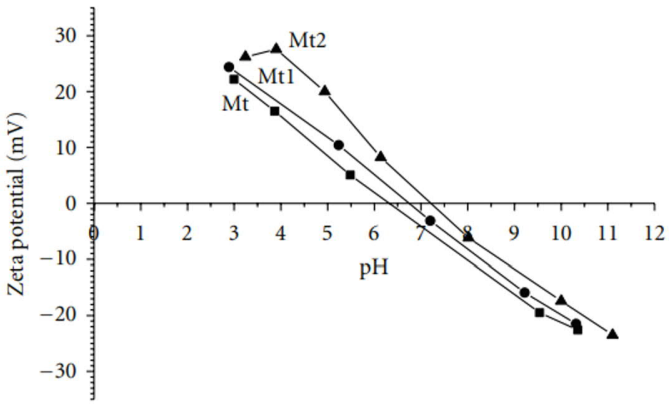

Figure 10. Relation of zeta potential and pH level. The Mt sample is of pure iron oxide particles the Mt1 and Mt2 are of iron oxide particles that are covered with TMAOH surfactant at different stages.

It might be beneficial to analyze the effect of different surfactants on the double layer thickness in follow-up experiments for this work, at least if there is interest in producing stable dispersions of cobalt particles prepared using a similar method to the one in this work. The dispersions could be done as well in water as in organic carrier fluid. The measurement should be done both for bare cobalt particles and for surfactant-covered particles of the same batch. At the same time, DLS could be utilized to determine how the surfactant affects the particle size. This way both the electric repulsion and steric hindrance, which prevent agglomeration from happening, could be uncovered.

4 Characterization

There are several characterization methods of interest concerning particle preparation. The following methods are used in this work: transmission electron microscopy (TEM), scanning electron microscopy (SEM) with an integrated analysis technique called energy-dispersive X-ray spectroscopy (EDS, also abbreviated EDX and EDXS), and X-ray powder diffraction (XRD). The chapter covers these techniques in detail. In addition, thermogravimetric analysis—mass spectrometry (TGA-MS), spectrophotometry, dynamic light scattering (DLS), electrophoretic light scattering (ELS), atomic absorption spectroscopy (AAS) as well as inductively coupled plasma atomic emission spectroscopy (ICP-AES) could be utilized in future research. These techniques are discussed briefly in the last section of this chapter.

4.1 TEM

In this study, one of the most important analytical methods used to characterize the product is transmission electron microscopy (TEM, an abbreviation also used for microscopes of this technology). TEM provides a means of visually observing the sample and its internal composition with high magnification and resolution. It is a great tool for analyzing small areas and does not require large amounts of sample matter. On the other hand, TEM is not an efficient analytical method to be used for larger surfaces. Prepared samples must be solid, partly electron transparent and sustain vacuum conditions. Conventionally, TEM is used for acquiring detailed information on morphology and crystallization. Even the smallest structures and phenomena can be detected, including atomic dislocations, grain boundaries, tiny precipitates, and magnetic domains. These microstructural features can be seen in the bright field and black field imaging modes. There is also available an imaging mode called selected area diffraction pattern (SADP). With SADP, TEM can be used to gain information about the crystal structure of the sample, in addition to morphological details obtained in modes

mentioned above. In this work, TEM was used to qualitatively analyze morphology, crystallization process and crystal phases, primal particles and agglomerate size distribution, agglomeration degree, and process of agglomeration.

TEM operates on the same basic principles as most microscopes: a focused beam of particles (or waves) is targeted upon a sample and then scattered particles or particles passed through a sample are registered on a film to form an image. The configuration and working principle of the TEM are illustrated in Figure 7. The numbering on the right side of the image correspondents to the following steps. Firstly, electrons are formed in an electron gun that accommodates a cathode, typically a tungsten filament. The released electrons are accelerated by an anode at high voltage (approx. 100-200 keV) in respect to the cathode. Secondly, the beam of electrons is focused to the specimen by electrostatic and electromagnetic lenses. Energized electrons either scatter or pass through the sample that has been prepared to be partly electron transparent. Thirdly, the spatial variation of the electrons transmitted through the sample is magnified using a lens system and the information carried by the electrons is visualized using a fluorescent viewing screen or charge-coupled device (CCD) camera.

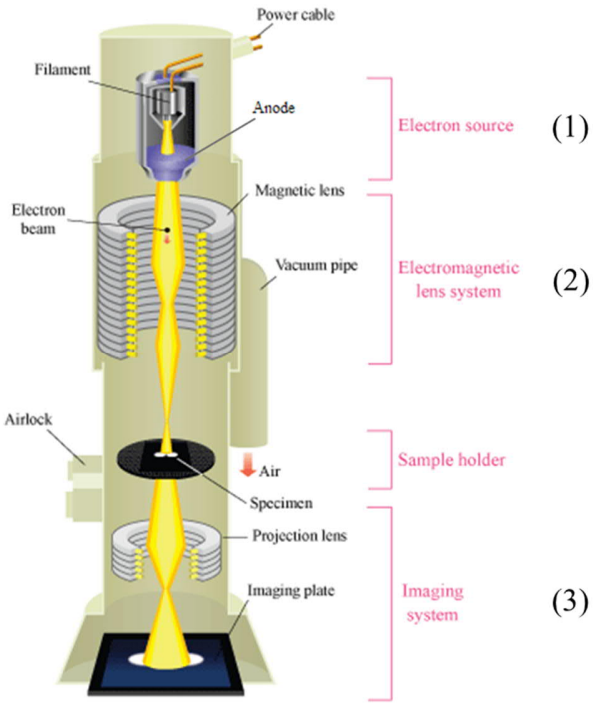

Figure 11. Parts and configuration of TEM, modified from a figure in [27].

4.2 SEM and EDS

Scanning electron microscopes (SEM) provide information on the surface features (topography) and composition. The exact type of information an SEM can produce mainly depends on the combinations of detectors. Basically all SEMs accommodate the Everhart-Thornley detector, a type of collector-scintillator-photomultiplier system, for registration of secondary electrons (SE) and backscattered electrons (BSE). Many SEMs detect also X-rays, i.e., they utilize energy-dispersive or wavelength-dispersive X-ray spectroscopy (EDS and WDS respectively). More uncommonly, SEMs can even analyze light emissions (cathodoluminescence, CL), electron beam induced current (EBIC) and transmitted electrons (scanning transmission electron microscopy, STEM). The

samples for the thesis were analyzed using SE and EDS technologies, therefore, they are covered in this chapter in more detail.

As in TEM, the electron source provides an electron beam that is accelerated and focused on a sample in SEM. Figure 12 presents the basic set-up of SEM with common detector type. The electron beam consists of high energy primary electrons (PE of approx. 20 kV). When these electrons hit the surface atomic layers (from less than 100 nm to 5 µ under the surface) of the sample under scrutinization, the sample begins emitting electrons and energy. The volume of the sample in which the emissions originate from within is called the interaction volume, and it differs for each emission type.

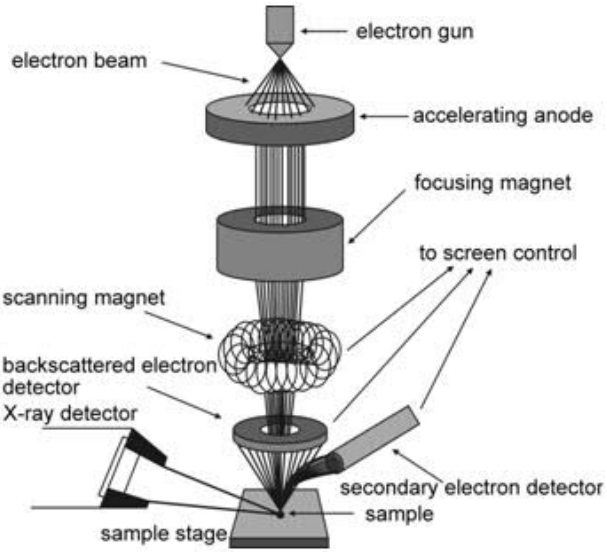

Figure 12. The set-up of SEM with BSE, SE and X-ray detectors as presented in [28].

The most relevant electron emission types consist of high energy backscattered and low energy secondary electrons. Their mechanisms of origin are illustrated in Figure 13. Backscattered (and reflected) electrons are used for composition contrast images and orientation imaging. On the other hand, secondary electrons are used for

producing high resolution 3D imaging of surface features in the conventional imaging mode. SEs are of low-energy (<50 eV) and originate from within a few nanometers below the specimen surface. The steeper is the surface, the larger the interaction volume and the shorter distance a secondary electron has to travel within the specimen matter to reach the surface. Therefore, steep surfaces (facing towards the detector) release more electrons and appear lighter than flat surfaces. This enables us to observe the three-dimensional shapes of a specimen. In the thesis, the SE imaging mode was used for acquiring images, analyses of morphology, growth mechanisms as well as size distribution of the particles and agglomerates, and general inspection of larger amounts of sample material at once compared to TEM measurements.

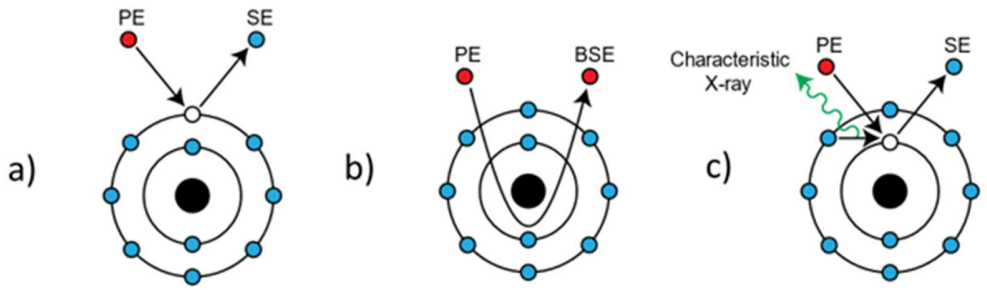

Figure 13. The origin of a) secondary electrons (SE), b) backscattered electrons (BSE), and c) characteristic X-ray emissions.

Besides electrons, the incident electron beam substance interaction generates heat and photons (visible light and X-ray emissions). The mechanism for emerging of X-rays characteristic to the substance is presented in Figure 13. If X-rays can be detected, they provide information on the chemical composition of the specimen surface in energy-dispersive X-ray spectroscopy (EDS) and wavelength-dispersive spectroscopy (WDS) imaging modes. This work utilizes EDS to semi-quantitatively determine the chemical (elemental) compositions in analyzed samples.

4.3 XRD

X-ray diffraction (XRD) can be used for phase identification of crystalline materials. In this work, XRD technique is used to identify whether our particles are of pure cobalt or do they contain significant amounts of silver, cobalt oxides or other crystalline impurities. An XRD instrument consists of an X-ray tube, a sample holder, and a detector. In the X-ray tube, a cathode is heated to release electrons, which are then accelerated to bombard the target material (Cu, Fe, Mo, or Cr). As an electron of high enough energy collides with and dislodges an inner-shell electron from an atom orbital of the target material atom, an outer-shell electron fills the vacancy and X-ray of wavelength characteristic for the target material is emitted. The X-ray emission is filtered to produce monochromatic radiation. Whilst, the whole X-ray spectra of any material consists of several components, typically only the most intense ones, K_α and K_β, are of interest. The most common target material is copper and X-ray wavelength the weighted average of Cu $K_{\alpha1}$ and $K_{\alpha2}$ emissions, Cu(K_α) = 1.5418 Å. The selected monochromatic radiation is collimated into concentrated beam of adjacent X-rays, which is then aimed at the sample at varied ϑ angles. The X-rays diffracted from the sample surface are then detected and counted. The identified diffraction peaks at known 2ϑ angles, i.e., the angle between transmitted and reflected ray, are converted to *d*-spacings in accordance with Bragg's law on constructive interference. Assuming the crystalline sample is properly prepared, i.e., finely ground and homogenized, the lattice planes will be randomly oriented. Therefore, the complete set of unit cell dimensions can be acquired, and crystalline materials identified through comparison of *d*-spacings with standard reference patterns. The relative count rates of diffracted X-rays are roughly proportional to concentrations in case several crystalline phases are present, so that they can be semi-quantitatively identified from the otherwise averaged composition data.

Bragg's law is the following:

$2d \sin\vartheta = n\lambda$ (7)

where d = one of the lattice spacings of the sample mineral

ϑ = angle between incident X-ray beam and crystallographic plane (surface tangent)

n = integer

λ = wavelenght of incident ray

Bragg's law describes the conditions that need to be satisfied for occurrence of constructive interference. Each side of the equation presents all possible differences in traveling distance of two parallel rays reflect of parallel crystallographic planes at angles where intensity maxima are detected. Figure 14 shows the geometry of diffracted X-rays: the difference in the traveling distance of the two rays is 2 times ($d \sin\vartheta$). The lattice spacing d can be derived from the Eq. 7. as other variables are known.

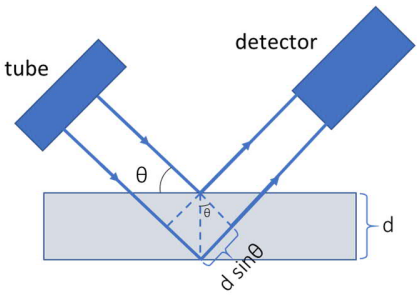

Figure 14. Not-to-scale representation of geometry of X-rays reflected from atoms on adjacent lattice planes.

4.4 Other Techniques of Interest

Techniques which were not utilized in this work but could be useful in the future research include thermogravimetric analysis—mass spectrometry (TGA-MS), spectrophotometry, dynamic light scattering (DLS), electrophoretic light scattering

(ELS), atomic absorption spectroscopy (AAS) as well as inductively coupled plasma atomic emission spectroscopy (ICP-AES) could be utilized in future research.

Thermogravimetric analysis—mass spectrometry (TGA-MS) could provide more information on the degree of oxygenation. If citrate-covered cobalt-cobalt oxide particles are heated under H_2 atmosphere, cobalt oxide gets reduced to cobalt, as oxygen reacts producing small gaseous molecules. These molecules, i.e., H_2O, CO, and CO_2, are identified and measured in the MS. Comparing this data to the mass—temperature data from the TGA, the oxygen/cobalt relation can be estimated in the actual particles (not including the citrate layer).

Spectrophotometry could be used to analyze the reduction reaction of Co in the formation and growth of Co particles. The conversion rate data can be acquired by taking samples of the reaction solution during the reaction. The relation of the initial and final Co^{2+} concentrations gives the actual conversion rate and can be used to estimate the effectiveness of given reaction procedure. This information can be used for optimization of the reduction reaction. On the other hand, the atomic absorption spectroscopy (AAS) and inductively coupled plasma atomic emission spectroscopy (ICP-AES) could give information on conversion as well as the Ag/Co relation. This could be done by dissolving prepared particles from the most promising reaction. The presumption is that all of the initial Ag, but only part of the initial Co amount, has reacted and is found in the particles. If the Ag/Co relation is acceptable, this reaction could be used for further refinement of the reaction procedure.

Dynamic light scattering (DLS) can be used to determine the average particle (or agglomerate) size both after the preparation of the particles and after the particle have been dispersed using large surfactants. The particles should have a narrow size distribution for reliable size determination. Electrophoretic light scattering (ELS) could

be used for estimating the dispersion stability by measuring thickness of the electric double layer.

5 Methodology

5.1 Synthesis of Cobalt Particles

Nine experiments were conducted in total. Of those experiments, products of six experiments were characterized. The reasons for not characterizing the three experiments are covered in the next chapter. The characterized experiments are grouped into two experiment series, Phase1 and 2, consisting of Exp1b, 2, and 3 as well as 5b, 6, and 7, respectively. The experiment series differ not only in the use of a nucleation agent but also in the experiment set-up in order to change the mixing method. In Phase1, stirring was performed with a magnetic stirrer typically used in the chemistry department, whilst, in Phase2, a mechanical stirring system was build using a custom-made glass rod with attached glass blades and a power drill. Images of the Phase2 set-up is shown in Figure 15 and Figure 16. The stirring system was changed to a mechanical one to protect Co from magnetization and, therefore, agglomeration. The instruments were mainly made of glass and some plastics which were washed with aqua regia when needed in order to limit the amount of impurities, especially cobalt-like magnetic chemical elements, Fe and Ni. The experiments were performed under N_2 to prevent Co from oxidizing.

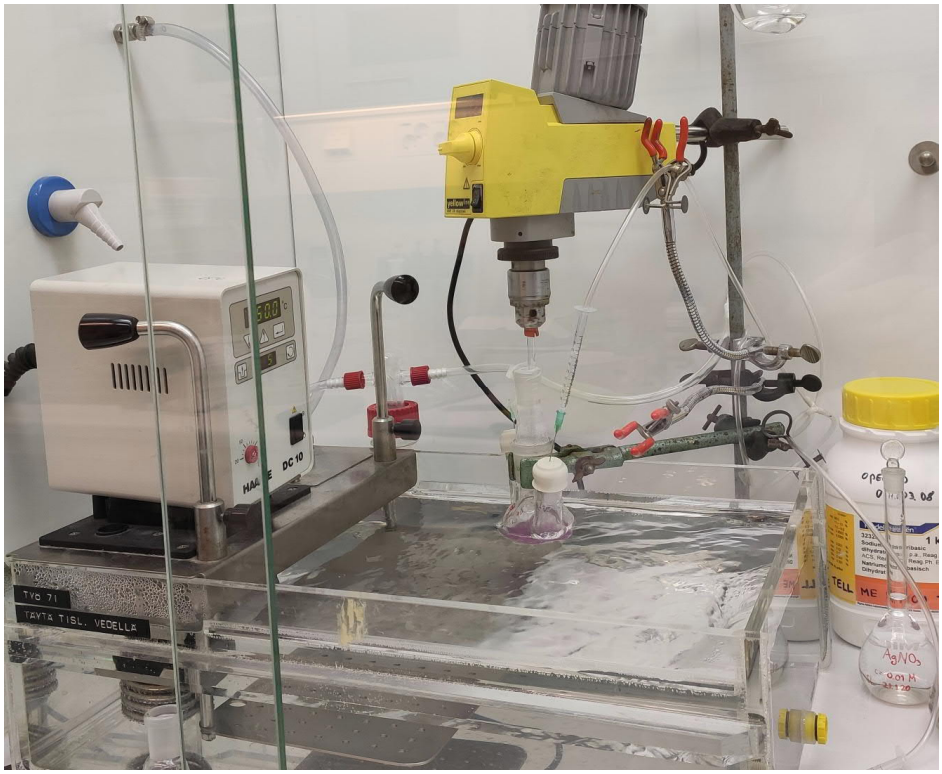

Figure 15. The key features of an experimental setup: a mixing system, N_2 tubing and bubbling system with a filter and humidifier and thermostated bath.

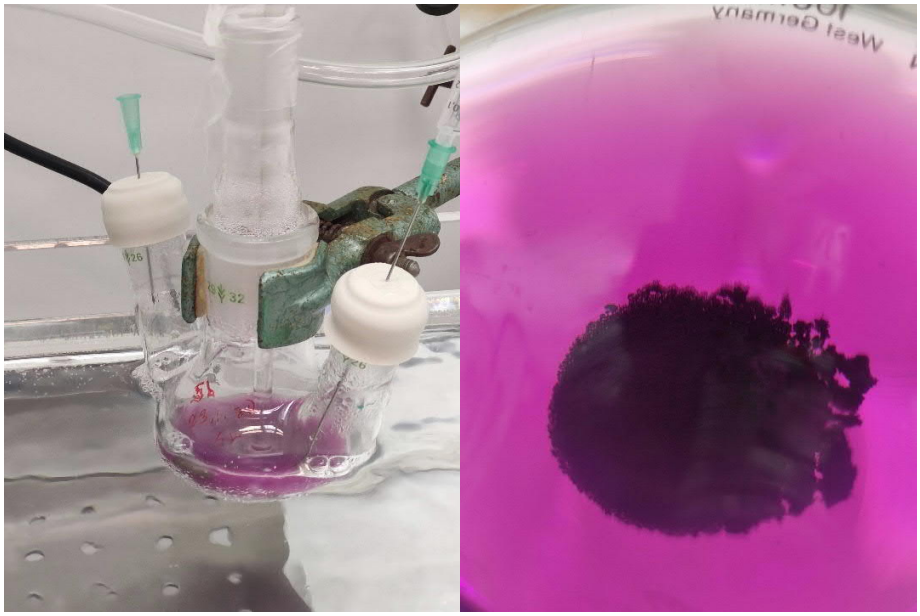

Figure 16. Close-ups of the Exp5b setup and formed particles.

The experiments were performed as follows. At first, all liquid reagents were treated with N_2 and thermostated to reaction temperature. $CoSO_4$, $AgNO_3$, and $Na_3C_6H_5O_7$ were added to MQ water, which volume was determined by subtracting the volume of other reagents from the total volume. NaOH was then used to adjust the acidity level of the solution until pH 14. In order to begin the reaction, N_2H_4 was slowly added to the solution. Table 3 shows the reagents and their corresponding concentrations for Exp5b, as an example. The initial concentrations of $CoSO_4$, N_2H_2, and $Na_3C_6H_5O_7$ were identical between all the experiments. The initial concentrations of $AgNO_3$ and NaOH are presented in Table 4 for all the experiments which products were characterized. Although the initial NaOH concentration varied, all reaction solutions had the initial pH level of at least 14, which was the maximum value of the pH indicator strips.

Table 3. Molar concentrations and amounts of reagents in Exp5b.

Chemical	*c* (mol/l)	*n* (mmol)
$CoSO_4 \cdot 7\ H_2O$	0.2	10
$AgNO_3$	$0.2 \cdot 10^{-3}$	0.01
$N_2H_2 \cdot H_2O$	5	250
$Na_3C_6H_5O_7 \cdot 7\ H_2O$	0.4	10
NaOH	0.32	16

$CoSO_4$ acted as a source of Co^{2+} ions that would be reduced to pure metallic cobalt particles. N_2H_4 was the reducing agent in the reaction. The function of $AgNO_3$ was to provide Ag^+ ions that reduce before Co^{2+} as silver is more noble in the galvanic series. Ag forms tiny particles and on their surface the reduction of Co occurs more easily. The molar ratio of Ag/Co affects the number and size of the particles providing means to control the reaction. In order to see how the ratio of Ag/Co affects the particles in the system used here, different ratios from 10^{-4}-10^{-2} were tested in this work. $Na_3C_6H_5O_7$ acted as a surfactant protecting the particles from oxidation and agglomeration.

The reaction conditions are presented in Table 4. The reaction temperatures were in the range of 25-65 ˚C. The temperature was 25 ˚C in Exp1a, 1b, 2 and 4. The Exp3 was conducted at the highest temperature of 65 ˚C. That reaction was initially extremely fast but gaseous products formed so fast that the solution could not be contained in the reaction flask. The flask needed to cool down a bit and reaction was continued at a lower temperature. Afterwards, the temperature was set at 50 ˚C, where it was fast enough but still controllable. In addition to temperature, an ending of the reduction reaction of Co can be attributed to a lowered pH level or consumption and evaporation of N_2H_4 during the reaction.

Table 4. The varied parameters and their values in the experiments.

Experiment	Temperature (˚C)	c($AgNO_3$) (mmol/ml)	c(NaOH) (mmol/ml)	Stirring method
1b	25	-	0.48	Magnetic
2	25	-	0.21	Magnetic
3	65	-	0.27	Magnetic
5b	50	$0.2 \cdot 10^{-3}$	0.32	Mechanical
6	50	$0.2 \cdot 10^{-4}$	0.32	Mechanical
7	50	$0.2 \cdot 10^{-2}$	0.32	Mechanical

The stirring methods scrutinized here were the conventional magnetic stirrer and a mechanical stirrer. All experiments in Phase1 were conducted using the former and the Phase2 experiments, the latter. Therefore, these groups are compared to each other to conclude how a magnetic field caused by the magnetic stirrer affects the growth of particles and which method is to be recommended for products to be developed for hard metal industry (both dry powder and suspended particles). The growth of particles was studied by TEM and SEM technologies for morphology and XRD for crystallization.

The effects of varying NaOH concentrations and, thus, pH levels are compared between Exp1b and Exp2. The corresponding concentrations are 0.48 M and 0.21 M at the starting point of the reactions. The NaOH concentration supposedly affects all the reaction species, including intermediate and byproducts, and the growth of the particles. More specifically, the elements observed were formation of intermediate product (a visible precipitate that disappears as the reaction progresses), pH level changes (color of the solution and 0-14 pH indicator strips), as well as morphology and particle size by utilizing TEM and SEM.

Effects of adding $AgNO_3$ as a nucleating agent are analyzed in more detail. Phase2 consists of a series of various relative concentrations of Ag^{+}/Co^{+2} between 10^{-4}-10^{-2}. The Phase2 experiments 5b, 6 and 7 are not only compared to each other but also to Exp2 and 3 from Phase1, which contain no $AgNO_3$. However, the comparison between the phases contains a larger amount of uncertainty as the temperature, stirring method and even the concentration of NaOH differ between those groups. The hypothesis is that the existence and relative concentration of a nucleating agent would have an effect on the reaction as a whole, and thus the particles, by bringing down the activation energy barrier of reduction of cobalt and forming a limited amount of core particles on which the cobalt gets reduced. First, these effects can be observed in terms of reaction rate: visually the progress by the color of the solution and the amount of bubbles being formed at a certain point in time as well as a change in the pH level. Second, the conversion rates can be compared visually by the amount of final particles and the solution color at the end of the reaction. Third, the particle size and agglomeration degree are estimated visually by TEM and SEM as well as observing movement and sedimentation speed as the vials where the particles are suspended in water are being shaken manually. Forth, morphology is inspected by TEM and SEM. Last, the chemical composition of the particles is determined by EDS and XRD.

The impact of temperature on the reaction is scrutinized mainly by comparing Exp2 with 3, but also by contrasting these experiments from Phase1 to the Phase2 experiments. The corresponding reaction temperatures are 25, 65 and 50 ˚C, of which the last being the same in the whole Phase2. Reaction temperature is supposed to affect the whole reaction as well as the products. Reaction rate, particle size, agglomeration degree, morphology and chemical composition are analyzed with the same methods than in the case of $AgNO_3$. Additionally, the crystallization is inspected by using SEM and TEM.

5.2 Characterization

2D visual inspection of Phase1 and 2 samples utilizing transmission electron microscopy (TEM) included examination of morphology, crystallization, particle size (primal particle and agglomerate sizes), agglomeration and phase boundaries. The TEM samples were prepared from diluted reaction solutions using modulated ultrasound to disperse particles evenly in the carrier fluid. A few droplets of diluted solutions were dropped on holey carbon copper grids and dried one or two days before TEM measurements. The Phase1 samples were analyzed using Tecnai 12 (120 kV accelerating voltage) and the Phase2 samples using Jeol JEM-2800 (200 kV) at 300k–5M magnifications.

3D examination and elemental analysis of Phase1 and 2 samples were conducted using a scanning electron microscope (SEM; MIRA3 TESCAN; 5 kV acceleration voltage; 100-10k magnification) and in-built energy dispersive X-ray spectrometry (EDS; 10 kV voltage) device. SEM provided a means to conveniently screen extensive areas of the samples and observe larger agglomerate structures as well as other morphological features. EDS was utilized to verify that the studied particles were of metallic cobalt. It was used in mapping mode for detecting chemical elements in selected regions and in

point-and-shoot mode for examination of a single particle. The point-and-shoot data from the coating covered stub was used as a reference for the data of particles. The samples were prepared using particles of which moisture was removed by vacuum drying at 40 ˚C. Dry particle powder was introduced onto epoxy (25:3 EpoFix Resin: EpoFix Hardener) on an aluminum stub. After the epoxy had hardened and dried the stub was coated with carbon (10 nm + 2-3 nm; in case of Phase1) or gold (Au/Pd 80/20, 5 nm; in case of Phase2).

The crystalline compound compositions and purity of Phase2 samples were determined qualitatively and semi-quantitatively by X-ray powder diffraction (XRD) analysis (PANanalytical X'Pert PRO; $CuK_{\alpha 1}$ radiation; 2ϑ angle range 10–100 ˚; 1-hour measurements). The samples were prepared by drying the washed Co particles in a vacuum oven at 40 ˚C and hand grinding them into fine powders using a mortar and pestle. The advantage of XRD was to be able to identify whether particles have oxidized under the surface and whether there are significant amounts of other crystalline impurities than oxides.

6 Results

As covered in Chapter 4 and 5, the particles were characterized qualitatively and semi-quantitatively by using the following techniques: TEM, SEM, EDS, and XRD. Scrutinization of the reaction products using these techniques and by visual inspection revealed few traces of oxidation. Therefore, it is probable that little or no oxidization had occurred during several weeks or months after preparation of the particles.

This chapter presents the most important data and findings of the thesis. The aim of the thesis was to develop a practical method of reducing metallic cobalt in an aqueous solution without an external electrical current. The effects of the stirring method, concentration of NaOH, nucleation agent and temperature on the reduction reaction and the product were under study. The experimental procedure and details of each experiment are presented in the previous chapter. As mentioned, the experiments and corresponding samples were divided to two phases accordingly: Phase1 comprising of Exp1b, 2, and 3 samples and Phase2 of Exp5b, 6, and 7. In addition to these six experiments, three others were performed (Exp1a, 4, and 5a) but not characterized due to several reasons: inferior reagent addition order, gas leakage, and crude-test nature. Therefore, these experiments are mostly not covered in this chapter, unless they provide special insights.

6.1 TEM

The information provided by TEM that were of interest are morphology, crystallization, primal particle and agglomerate size, agglomeration, crystal phases, and signs of oxidation. In general, TEM can be used to inspect smaller particles or larger wholes in more detail than SEM. Other uses for TEM are listed in Chapter 4. The variables, compared experiments, and results related to information available from use of TEM

as the characterization method based on the abovementioned plan are described in the following paragraphs. The scrutinized variables, of which effects can be seen in TEM images, are the following:

1. Stirring	Phase1 vs. Phase2,
2. Initial NaOH concentration	Exp1 vs. Exp2,
3. Existence and initial concentration of $AgNO_3$	Exp5b vs. Exp6 vs. Exp7 vs. [Exp2+Exp3],
4. Temperature	Exp2 vs. Exp3 vs. Phase2.

The values of the variables for each experiment were presented in Table 4 in the previous chapter.

The possible effects of the stirring method (magnetic or mechanical) under inspection were growth, morphology, and crystallization. The details of the experiment set-up were covered in the previous chapter. Figure 17 shows a common feature among the Phase1 samples that many particles are elongated, meaning that the growth process has been guided by the magnetic field of the stirrer. Interestingly, there are only round particles in the Exp2 sample for an unknown reason. It could be linked to the smaller ionic strength and concentration of NaOH compared to reaction rate. It is also possible that the magnetic stirrers used in different Phase1 experiments were not identical in spite of similar size and shape, or that the stirring had otherwise any effect, or that the Exp2 sample was not representative of the batch. It is also noticeable that all samples contained round particles. All Phase1 samples contained highly ordered spherical structures, secondary particles, which are formed of much smaller primary particles, as can be seen in SEM images in the next section.

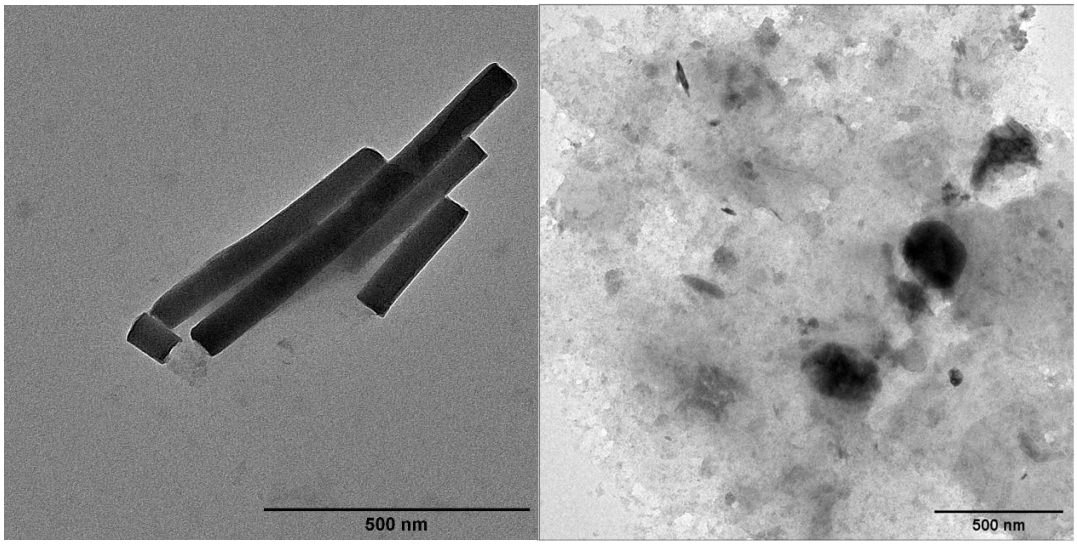

Figure 17. TEM image of rod-shaped (on the left) and rounded particles (on the right) in Exp3 and Exp2, respectively.

The Phase2 samples showcase small and medium-sized, rounded primal particles of less than 20 nm in diameter, larger crystals (hundreds of nm) as well as huge dendrites (1-10 µm). Examples of crystallized cobalt particles are presented in Figure 18.

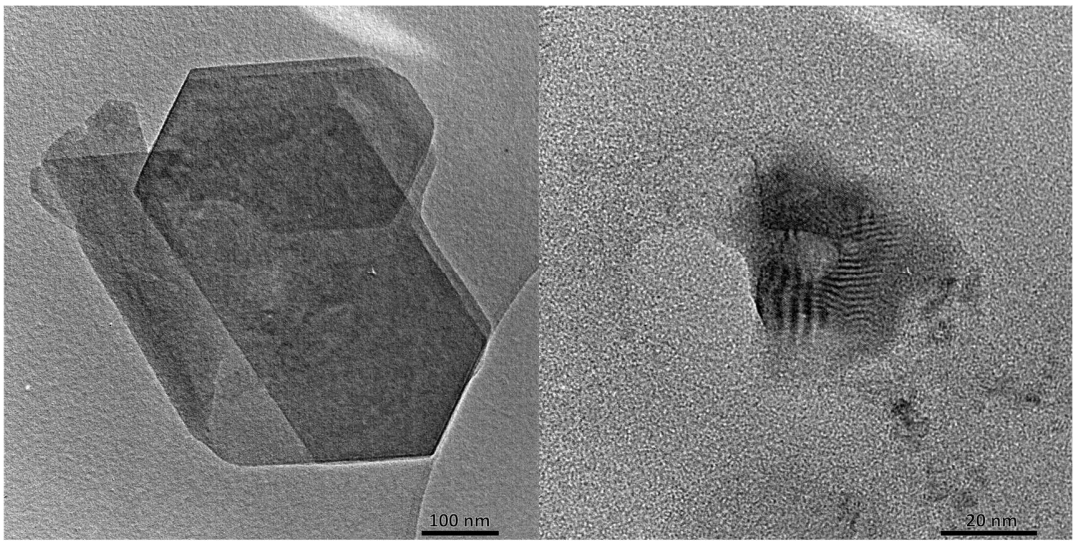

Figure 18. TEM images of Exp5b imply a crystalline structure by larger particles having sharp corners and smaller ones showing visible electron diffraction patterns from the crystal lattices.

The effect of NaOH concentration, i.e., initial pH level, was examined in terms of the reaction products, including intermediate and byproducts, and growth of cobalt particles. The growth process during the reaction could be analyzed by examining morphology and size of the particles with SEM after the reaction. If the reaction, especially the nucleation stage, was to go through intermediate product, a NaOH-derived ligand could be acting as a catalyst enabling the intermediate reaction to take place, which precedes the reduction reaction step. This could partly explain why the reaction only happens at very high pH levels (minimum pH 12.6 according to [19], although seen at pH 11 in the initial test Exp1a), as the coordination complex to form, the OH^- ion concentration needs to be high enough. In that case, OH^- ions would be required even though they are not consumed at the coordination complex stage. The consumption of OH^- ions happens during the cobalt reduction. In other words, OH^- ions can have a catalytic nature in the stage of the reaction but are normal reagents in the second stage. Consequently, higher initial NaOH concentration could potentially result in faster reaction rate, higher yield or conversion and smaller particle size.

The comparison of different initial NaOH concentrations was done between Exp1b and Exp2, which had otherwise similar initial reagent concentrations. Unfortunately, no conclusions can be made for the effect on reaction time. Exp1b stopped unintentionally because non-humidified N_2 gas flow (for creating an oxygen free atmosphere) had dried out the solution. This problem occurred due to low reaction temperature in the first experiments causing the reaction time to be several days instead of few hours, that was anticipated based on the literature. This problem was fixed after reaction 1b by using humidified N_2. Examining all reactions, it seems, however, that reaction temperature has more significant effect on the reaction time than NaOH concentration.

Additional notion on the NaOH concentration is that an initial test Exp1a, which was identical to Exp1b except for the order of how reagents were added, was not allowed to continue till the end and of which particle product was not analyzed. Nonetheless, an important observation was that the reduction reaction took place before adding any NaOH. Reason behind this was that, according to literature, the reaction cannot happen under pH level 12.6. The pH of the reaction solution was around 11. This indicates that the reaction can take place at somewhat lower pH levels even at a very low temperature. The main difference between the experiments of this work and the ones in the literature was probably different concentrations of other reagents, especially the high relative amount of N_2H_4 to Co^{2+} ions. Discovering the limits of reaction conditions is important in terms of understanding the nature of the reaction. However, lower (initial) pH level and temperature cause the reaction to be too slow for industrial applications. Moreover, if the pH level is allowed to decrease due to OH^- ion consumption in the reaction, i.e., not maintained constant by NaOH addition, the conversion of cobalt will probably be on the lower side. Low conversion could be seen in this work indirectly with pink color of the solution after the reaction had stopped.

As mentioned earlier, there was a remarkable difference in the morphology of the Exp1b and Exp2 samples. The particles of the Exp1b sample were elongated and the growth had strongly been guided by the magnetic field from the stirrer as can be seen in Figure 19. On the contrary, Exp2 particles were almost perfect spheres even though the same stirrer was used. NaOH concentration (and lower ionic strength) might have an effect on the shape and size of the particles. In theory, larger ionic strength of the reaction solution decreases the electric double layer thickness and increases the size of particles (both primary particles and agglomerates). Spherical particles have probably been formed in a diffusion-controlled reaction, so maybe the mass transfer of OH^- ions has not been able to keep up with consumption of the ions in the reduction reaction.

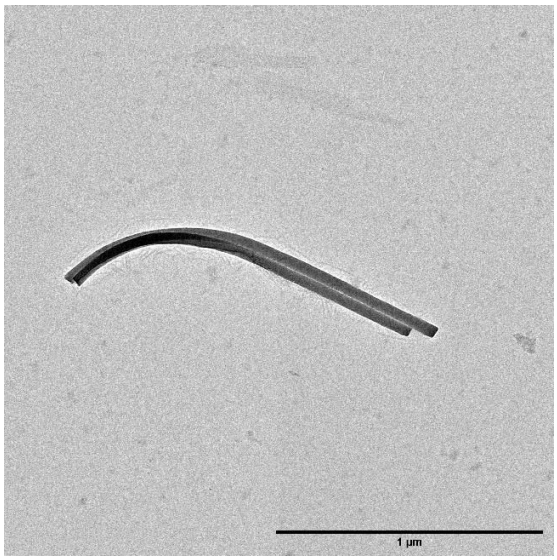

Figure 19. TEM image of elongated Exp1b particles shaped by the outer magnetic field.

The effects of existence $AgNO_3$ and relative concentrations of Ag^{+}/Co^{+2} were done between Exp5b, 6 and 7 as well as Phase1 (especially Exp2 and 3). The last one, the comparison between Phase1 and 2 as in existence of $AgNO_3$, contains a larger amount of uncertainty as the temperature, stirring method and even the concentration of NaOH differ between those groups. The effects of $AgNO_3$ were predicted to be seen in the reaction as a whole, and thus, the particle size and agglomeration degree, as well as morphology.

All Phase1 samples had both small primary particles of less than 20 nm in diameter and huge particles. Nevertheless Exp7, which had the highest concentration of $AgNO_3$, had relatively much higher number of small particles than Exp5b and 6. Moreover, the primary particles were the tiniest of all: 1-3 nm in Exp7, approx. 20 nm in Exp5b, and less than 5 nm in Exp6. The size and shape of the agglomerates of the particles could be scrutinized visually by shaking the vials containing the reaction products by hand or using ultrasound. Thus, one could observe how fast and well particles disperse and

then settle to the bottom. The Exp7 particles clearly had the finest composition, and that experiment seems promising for applications which require stable dispersed cobalt solutions and could be used as a starting point for that kind of product development.

On the other hand, Exp7 had some large dendritic particles which were not seen in any other experiment. Comparison of the two types of Exp7 particles is presented in Figure 20. Large particles in the Exp7 sample are dendritic but the detailed structure has fused together via sintering to form rounded branches as described in Section 3.1 Definitions of Dispersion Stability. It is also possible that the large particles have formed of rounded particles by agglomeration, but this is unlikely because the structure would not be branch-like as it seems to be in Figure 20. Instead, some of the primary particles have taken a dendritic shape in the growth stage. For some reason, cobalt has reduced faster on dendrites than nano-scaled particles. The dendritic shape implicates fast growth limited by mass transfer of cobalt ions (diffusion).

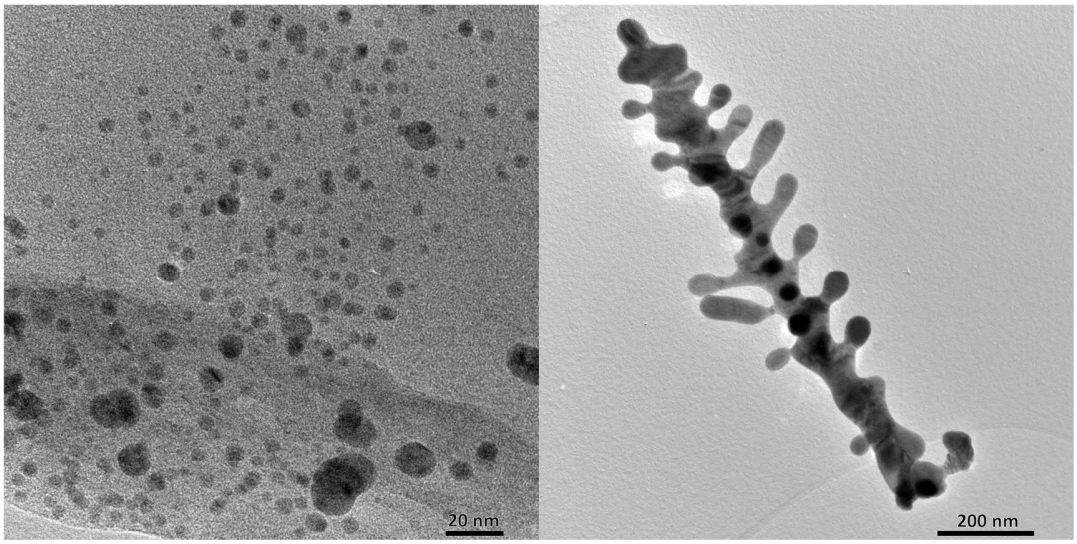

Figure 20. TEM image of tiny particles and a large dendrite in the Exp7.

It is rather surprising that the dendrites have formed in Exp7 which has the highest Ag^{+}/ Co^{2+} ratio. Although, mean particle size seems smaller in Exp7 than other Phase2 experiments. This could accelerate Ostwald ripening. In that case, part of the primary particles would actually have dissolved and become consumed by growing dendrites. Another hypothesis is that the dendritic growth happened due to concentration differences when there was a mixing problem in the beginning of the reaction. Two different sizes and shapes could be formed as a result of two types of nucleation: the conditions allowed formation of both silver and cobalt nuclei in different parts of the reaction flask. This kind of scenario is possible if a solution depletes of silver ions when there is still a lot of cobalt ions unreacted. However, this is unlikely as there were more silver ions in Exp7 than other Phase2 experiments.

A clear linear dependency could not be seen with the amount of used $AgNO_3$ in this work as no experiments produced particles with a narrow variation in size. In contrast, Balela [16] could produce a linear dependency between the inverse of $AgNO_3$ concentration and diameter of cobalt particles in her cobalt particle experiments utilizing the polyol process covered in the sections 2.3 and 2.4. Furthermore, it is possible that the inverse proportionality exists only in certain conditions or in a narrower $AgNO_3$ concentration range. It is worth noting that no one has thoroughly researched this relationship in aqueous media.

Furthermore, a linear dependency of the inverse of $AgNO_3$ concentration and Co particle size can be seen when estimating the medians of particle size distributions in Phase2. In Exp6, with smallest $AgNO_3$ concentration, majority of the particles are over 200 nm; in 5b, with a medium concentration, majority of the particles were either around 20 nm or 100-400 nm in size, and in Exp7, with the highest concentration of $AgNO_3$, majority of the particles were less than 5 nm. Even though, the particle size median might somewhat be relative to the $AgNO_3$ concentration, the mean particle

size seems not. Considering wolfram carbide as the end product, for which the particles would be melted, it is finally the mass of cobalt that matters. For example, even though over 95 % of the Exp7 particles might be small nanoparticles, it is still possible that most of the mass of the cobalt product is in the bigger particles of >100 nm in the largest dimension. To be precise, the mean particle size was not determined in this work, but this could be done with the dynamic light scattering method (DLS) in the future research. Accurate measurements would, however, require more defined preparation process in order to receive particles with a narrow size distribution. It is important to acknowledge that there is only three measurement points (three experiments with varying $AgNO_3$ concentration) and, therefore, no reliable conclusions on the $AgNO_3$ concentration and Co particle size can be drawn anyway.

In Phase1 with no $AgNO_3$ added, particles are mostly large and elongated. The long size has probably been influenced mainly by slow growth, caused by low temperature, and slow nucleation of cobalt as well as guidance from the magnetic field of the stirrer. All these are different from the conditions and following growth process of the particles in Phase2. It is not possible to directly assess effects of $AgNO_3$ on the differences in size and shape of the particles between Phase1 and 2 reaction conditions being so different.

The mean particle size cannot be easily determined using TEM, as the samples do not represent the actual size distribution reliably. In the future, the particle size could be estimated by using DLS, as discussed in Chapter 4. Then sample preparation from the product mixture of water and particles would not affect the accuracy of the results. Although, DLS only gives us the mean particle size. Furthermore, due to the large variance in particle and agglomerate sizes, the results would not be totally reliable. Large particles block smaller ones. As some agglomerates seem hundreds of times

larger in diameter compared to primal particles, determining the precise size distribution is challenging using most common techniques.

Lastly, TEM images can show details that indicate oxidation. All Phase1 samples (Exp1b, 2 and 3) showed particles with a surface layer of lighter color which could be cobalt oxide. However, the layer might also be of citrate, some leftover reagents, or a product from side reactions, as the Phase1 particles were not washed before sample preparation for TEM measurements. The Phase2 particles were washed using MQ water before any type of sample preparation. Therefore, only the Phase2 samples should be used for assessing possible oxidation. The Phase2 samples showed only thin lighter-colored layer of presumably oxidized cobalt. For instance, one large Exp7 dendrite of 1200 nm in length had rounded branches of 20-80 nm in diameter. The dendrite was covered with approx. 2 nm thick lighter-colored layer. Another rounded dendritic particle formation of 700 nm in diameter had an oxidized layer of 2-6 nm. Oxidized layers had probably formed after sintering of branches' detailed structures. Oxidation might have occurred even after TEM sample preparation, when particles were isolated from the liquid phase and left to dry in air on the TEM grid. Anyway, the relative amount of oxidized cobalt was very small. There was not visible oxidation in particles smaller than 100 nm in diameter.

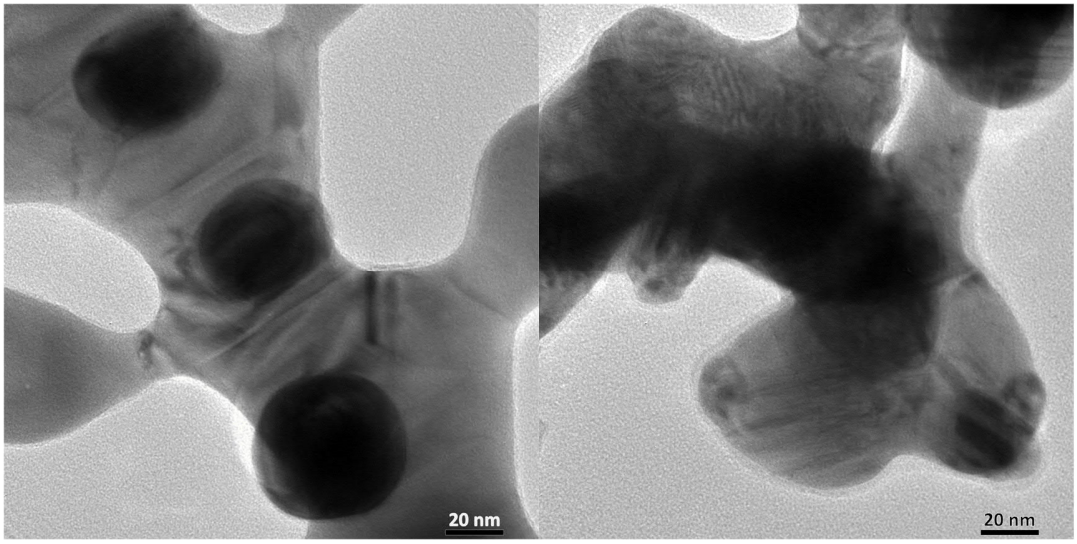

Figure 21. TEM images where the oxidized layers on Exp7 largest dendrites can be seen as a lighter outline on the particle surface.

6.2 SEM and EDS

Effects of the stirring methods on morphology was compared between Phase1 and Phase2. The main reason for potential morphological differences was assumed to be presence or lack of a magnetic field. However, different stirring methods can also affect the growth and final morphology of the Co particles and particle clusters due to different mixer geometry and surface properties (plastic or glass). Interestingly, SEM imaging showed cauliflower-like formations and round clusters in Phase1, in contrary to the smaller-scale TEM. Only the Exp3 sample had a particle of around 350 µm in length, of which growth had clearly been shaped by the magnetic field, even though other particles of the same sample were rounded, as seen in Figure 22. Although, absence of larger, elongated particles in other samples may have been caused by the samples not being representative, the one in the sample Exp3 should be considered as an interesting abnormality. The Exp2 sample had the most perfectly shaped spheres. The corresponding TEM sample contained no elongated particles, which might affect the three-dimensional shape of the secondary (and tertiary) particles that show in the larger scale of SEM.

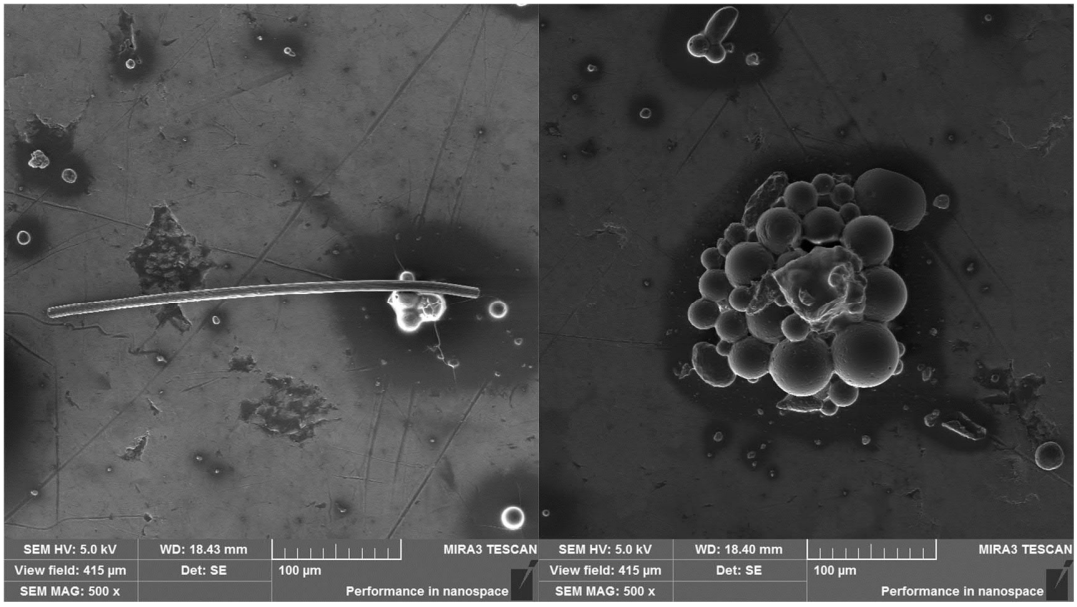

Figure 22. SEM images of an elongated particle and rounded or spherical particles in the sample Exp3.

The Phase2 particle agglomerates constitute of cauliflower-like formations, as seen in Figure 23. In the case of Exp5b, the surface texture was porous and sponge-like as seen in Figure 24. No elongated or spherical shapes could be seen in the Phase2 samples. It is notable that the SEM sample preparation had been unsuccessful considering that the particle substances had absorbed too much glue into themselves. This made it hard to see details outside protruding parts of the formations.

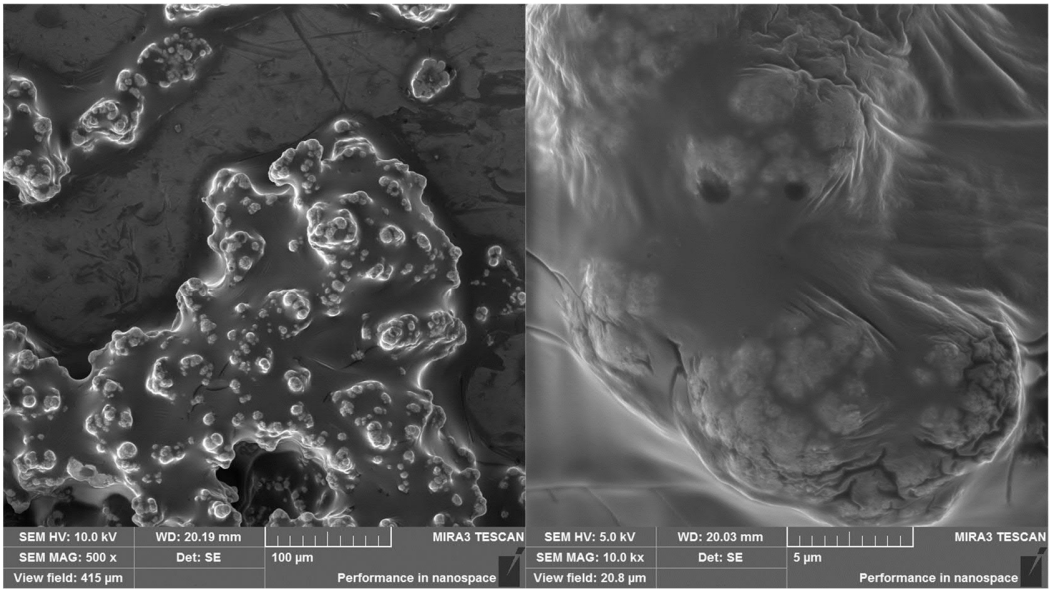

Figure 23. SEM images of glue-covered particles and a close-up of the cauliflower-shaped, agglomerated structure of the Exp6 sample.

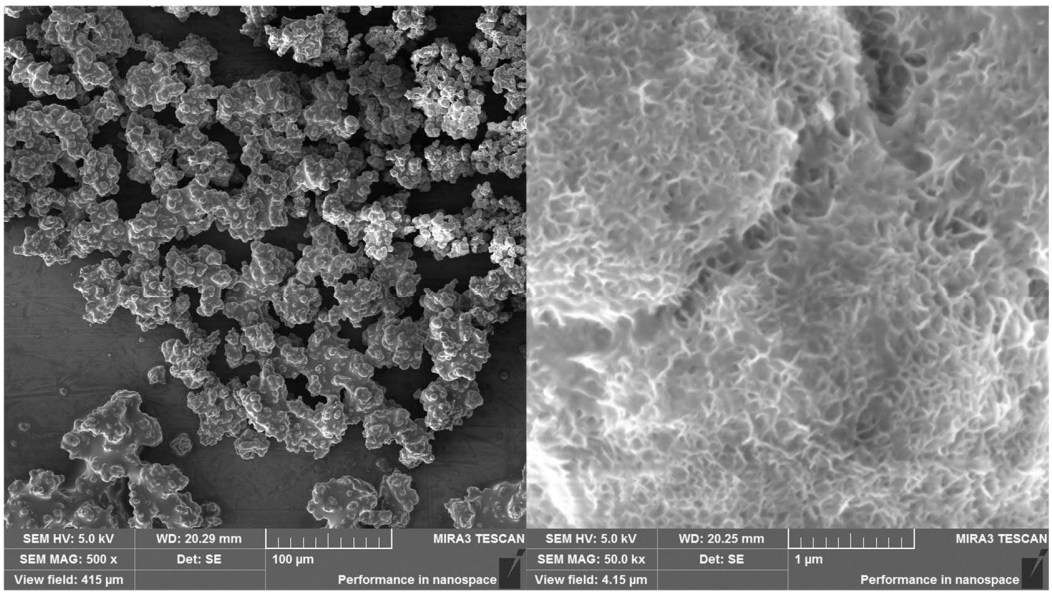

Figure 24. SEM images of Exp5b particles with a sponge-like structure shown in the right image.

The effects of the NaOH concentration (~pH) on morphology and particle size was examined between Exp1b and Exp2. In the Exp1b sample, the secondary particles are

more scattered and the primary particles form smaller clusters than in the Exp2 sample. There are practically no separate primary or secondary particles but tight formations in the Exp2 sample. Almost perfect spheres have been formed in Exp2. One can also see areas in the Exp1 sample where sphere-like particles have partly formed. Given that the Exp1b reaction had probably stopped prematurely as the reaction solution had dried, one could speculate whether it had ended with more round particles had the reaction had more time.

The particles sizes and morphology were analyzed once more by comparing the Phase2 samples regarding the concentration relation of Ag^{+}/Co^{+2} as well as comparing the Exp2, Exp3 and Phase2 samples in regarding the temperature. All Phase2 samples contained around 5-10 µm spherical secondary particles, which formed tertiary structures on tens of µm in diameter. These tertiary structures then formed loose clusters of hundreds of µm. There were no significant differences in size or morphology between the Phase2 samples at SEM scale. This means that the Ag^{+}/Co^{+2} relation did not seem to have any effects on micrometer scale, at least in these conditions. However, one could see differences in the size and morphology in the TEM measurements. Moreover, fineness of the particles, short-term dispersion as well as settling speed differed between the samples as seen by naked eye while disturbing the reaction solutions using ultrasound or by manually shaking reaction flasks or vials. In contrast to piled particles seen in the Phase2 samples, the Exp2 and Exp3 TEM samples consisted of spherical particles. The highly spherical nature seems not to result from differences in temperature or magnetic field. Therefore, it is possible that this is linked to the absence of $AgNO_3$ in these experiments, but it could also be related to some unknown factor.

The ionic strength has an effect on the particle size as covered at the end of Chapter 3. A high ionic strength increases the particle size through agglomeration as thinner

electric double layer does not hinder agglomeration process as well (Hosono et al., mentioned in [26]). However, it is hard to determine the ionic strength during the actual stage where particles form and as the nucleation and growth phases take hours or even days, it is even harder as the ionic strength changes all the time. Even before the main reaction takes place, part of N_2H_4, for example, reacts with water forming $N_2H_5^+$ and OH^- ions and some will evaporate out of the solution, so the exact ionic strength is unknown. In case of Exp1b and Exp2, Exp2 has a significantly higher initial concentration of N_2H_4 than Exp1b but concentration of NaOH half the one of Exp1b. As can be seen in Figure 25, the size of spherical tertiary structures in the Exp1b SEM images caps at 25 µm, while the largest Exp2 tertiary structures are close to 100 µm in diameter. It is notable that the size of the spherical particles varies hugely from 10-100 µm in the Exp2 sample. As the ionic strength is unknown during the stages of the main reaction, its effect on the mean or maximum particle and agglomerate size is impossible to estimate in this kind of experiment setup, unfortunately.

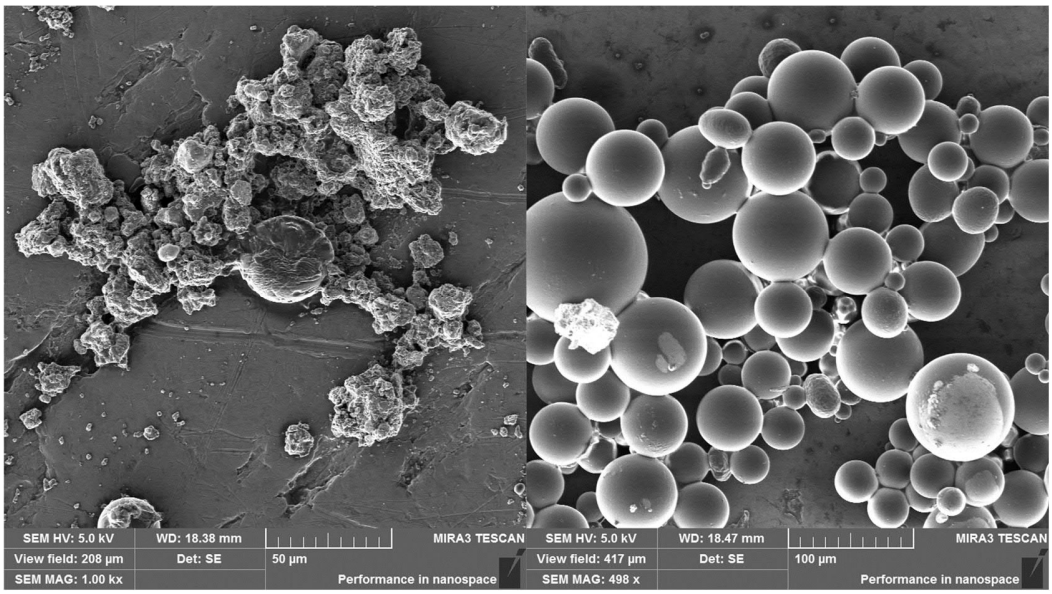

Figure 25. Comparison of spherical particles of Exp1b (left) and Exp2 (right) by SEM imaging.

The elemental and semi-quantitative analysis with EDS showed no impurities of significant amounts. The impurities detected were presumably from the stub, glue, and coating. It could be verified that the particles were of metallic cobalt. Table 5 shows the semi-quantitative results of a Exp7 particle taken in the point-and-shoot mode. The Exp7 reaction solution had the largest initial Ag^{+}/Co^{2+} ratio of 1/100. The Co/Ag atomic ratio is of the same magnitude as the initial Ag^{+}/Co^{2+} ratio (0.0055 and 0.010, respectively). However, there is a lot of uncertainty in the case of Ag in the Exp7 sample. The characteristic radiation of palladium from the Au/Pd 80/20 coating is close to the characteristic radiation of silver: Pd L_{α} being 2.838 keV and Ag L_{α} 2.984 keV in energy. Interestingly, the reference data of the stub shows 2.07 wt% and 0.38 at% of silver. Nevertheless, the relative amount of Ag seems low in the Exp7 sample and no Ag was detected in Exp5b and 6 particles chosen for the point-and-shoot measurement.

Table 5. Semi-quantitative EDS results of Exp7.

Element Line	Element Wt. %	Atom %
C K	0	0
Al K	1.22	2.85
Co L	86.2	92.24
Ag L	0.88	0.51
Au M	9.34	2.99
Pd L	2.37	1.4

6.3 XRD

XRD was used as a characterization tool to examine the chemical composition qualitatively and semi-quantitatively. XRD was only used for Phase2 experiments to observe any differences in compositions of crystallized structures that could be attributed to varying concentrations of $AgNO_3$ in the reactions. For example, any benefits of using higher concentrations of $AgNO_3$ might be invalidated if there were unacceptable levels of silver in the product for applications in the hard metal industry. The measured data is presented in Figure 7. The reference data for the Co (hcp) and Ag (fcc) reflections has originally been presented in [29] and [30], respectively. All Phase2 samples are of metallic cobalt (hcp) and no sample contains significant amounts of crystalline oxides. It seems that the samples are pure Co, except for Exp7. The Exp7 data shows a small reflection at around 38.3 ˚, which indicates the presence of Ag. According to the reference data, other reflections of Ag are relatively small, share the same 2ϑ angles with hcp Co or have a 2ϑ angle of over 100˚, which was outside of the measured range. This means that they cannot be used to indicate the presence of Ag. The Exp7 reaction solution had the largest relative Ag/Co concentration of 1/100, whilst the others showing no signs of Ag in XRD had relative concentrations of 1/1000 and 1/10,000. One could speculate if the reflection at 38 ˚ is caused by trigonal $Co(OH)_2$, but it is unlikely as there should be an even higher intensity reflection at 19 ˚, which is not seen in Figure 26 [31]. Therefore, it can be concluded that none of the samples show any crystalline impurities except for small amount of silver in the Exp7 sample and that the particles had not been notably oxidized before, after or during the sample preparation. A typical sample preparation could have easily oxidized the particles. The oxidization was probably avoided by not grinding down the samples, which is usually performed to increase the precision, and minimizing the time that the particles and prepared samples spent in oxygen-containing atmosphere.

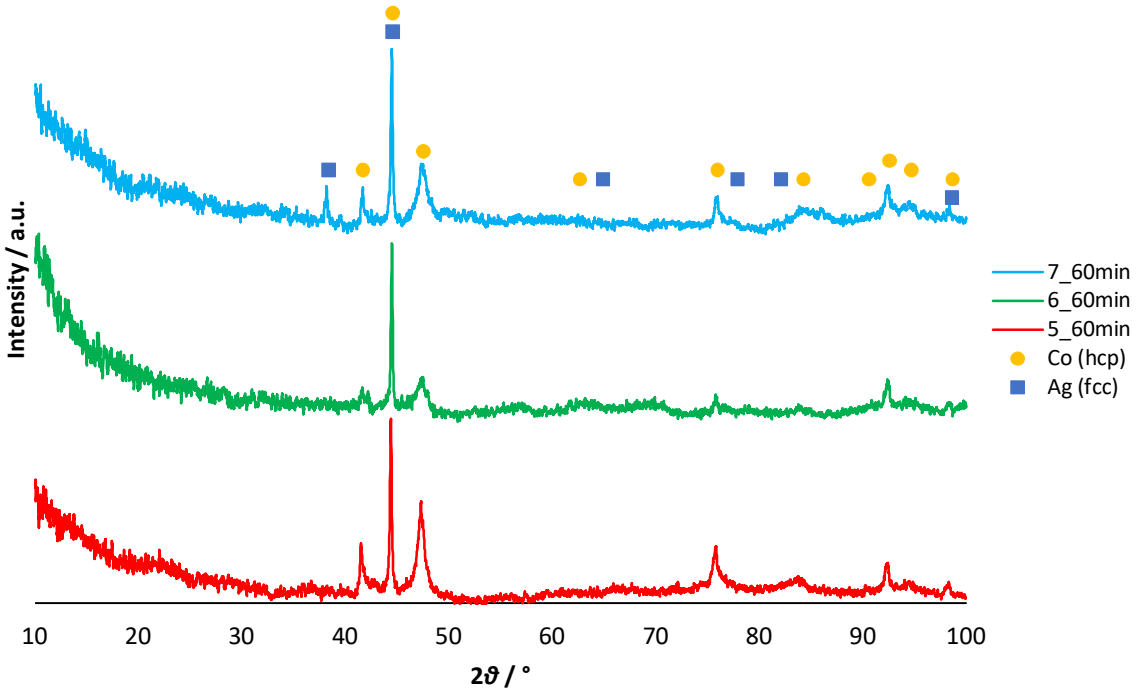

Figure 26. XRD patterns of samples from Exp. 5b, 6, and 7 with reference points marking reflections for Co (hcp) and Ag (fcc) crystal structures, originally presented in [29] and [30].

6.4 Other observations

The progress of the reduction reaction and the structure and form of the particles can be analyzed also with general laboratory observations. The progress of Exp3 is presented in Figure 27. In the case of cobalt, the changes in the oxidation state can be seen by naked eye as the color of the reaction mixture changes. Changes in color refer to the reaction mechanisms as well as how much of the cobalt is yet to react, i.e., the cobalt ion concentration. The blueish hue after adding NaOH indicates formation of a coordination complex between a cobalt ion or cobalt compound and hydroxide ions, as seen in Figure 27a). Furthermore, the reaction mechanism and the progress of the reaction are indicated by the amount of gas bubbles being formed at a certain point in time as well as a change in the pH level. On the other hand, the yield of the reaction

can be estimated by the amount of the particles and the conversion by the color of the solution after the end of the reaction. Moreover, the effects of $AgNO_3$ in the particle size and agglomeration degree can be seen in the proneness for dispersion and sedimentation speed when the vials containing the purified particles suspended in water are centrifuged, treated with ultrasound, or shaken manually. The two latter were covered in previous sections. Centrifugation, however, did not show any difference in the samples, as all particle products settled quite fast even without it. Nonetheless, it could be a quick way to test the fitness of dispersions in potential future experiments on dispersion stabilization.

Colors of solutions and precipitates (intermediate products and cobalt particles) varied in the experiments, for the order of chemicals added was different, including the adjustment of the pH level with NaOH. Also, the relative concentrations of the reagents were different in search of the best chemical procedure. These variations in colors of the solutions and formation of a precipitate give us hints of how the reagents coordinate in water and what intermediate products (precipitates) are formed. However, the following was observed in every experiment. After adding N_2H_4, the solution started getting lighter in color and whitish precipitate appeared, as seen in Figure 27b). The solution was not clear but milky due to those particles and the volume of tiny gas bubbles forming (from reactions of N_2H_4). Later, light-colored intermediate product disappeared and dark grey or black particles emerged (Figure 27c)). As the main reaction progressed, the solution became clearer and light pink and the amount of dark particles continued to increase (Figure 27d)).

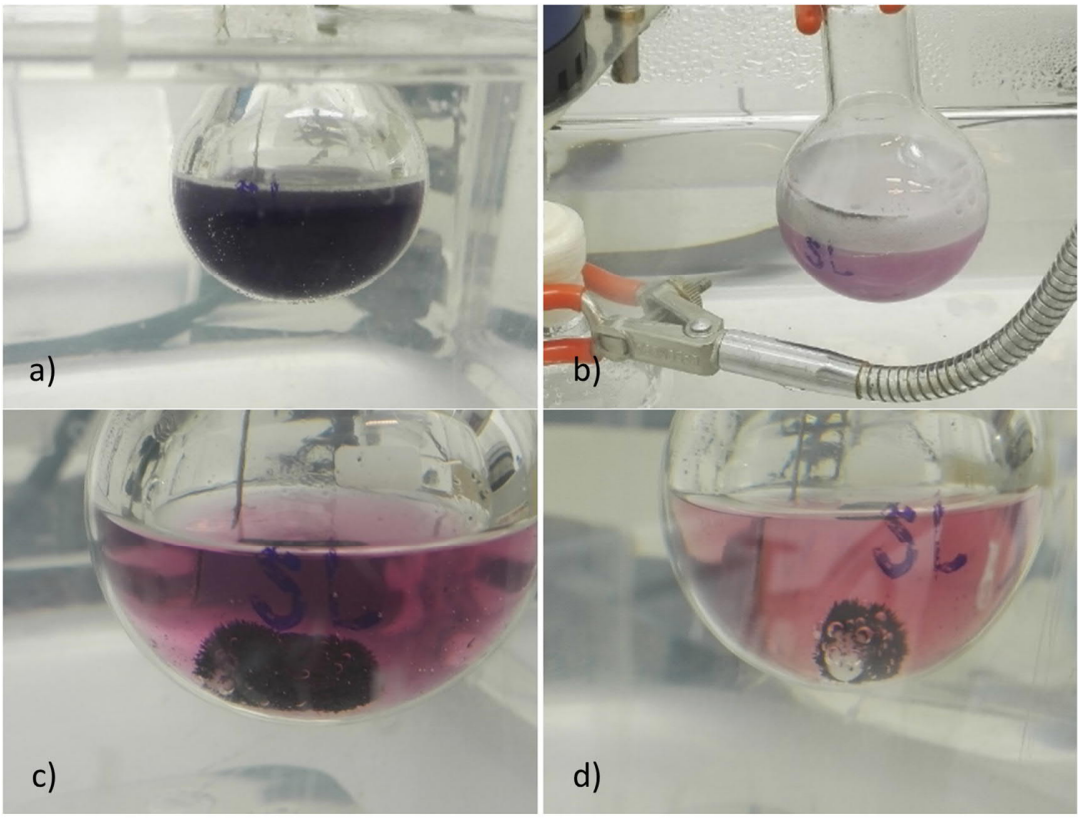

Figure 27. Colors of the Exp3 solution: a) All reagents had been added except N_2H_4, b) N_2H_4 has been added, c) A couple of hours later most of the Co has reacted, and d) Next day the reaction has stopped.

7 Discussion and Conclusions

The aim of this thesis was to be able to reduce cobalt ions to metallic particles in an aqueous solution. This was to be achieved without significant oxidation of the particles, i.e., without formation of cobalt oxide. To study the reaction, a system was built with a mechanical stirrer, controlled temperature, and nitrogen atmosphere. The motivation for this work was to create basis for a novel way to produce cobalt particles in a more sustainable way compared to processes in organic liquids. The ultimate goal would be to develop a method to preserve cobalt particles in a stable dispersion to be used in the hard metal production, instead of dry powder. The methods to prepare a stable cobalt dispersion in water were examined only through the literature as the COVID-19 pandemic limited the possibilities to work in the laboratory. The experimental work that could be performed was based on two hypotheses, which are discussed below.

The first hypothesis was that the reduction reaction and preparation of particles are possible in mild temperatures with similar reagents proven to work in organic solutions. This hypothesis was confirmed most probably due to extremely basic conditions and high concentration of the reducing agent N_2H_4 in this work. The second hypothesis was that the reaction, especially the particle size, can be controlled with the use of $AgNO_3$ as a nucleation agent. This could be partially confirmed by analyzing particle sizes with electron microscopes and scrutinizing particles by naked eye. However, the difference between the Phase2 products was not particularly large and the series of three experiments can be considered only as limited evidence.

This work had some limitations and shortcomings. Firstly, the small number of experiments lessen the reliability of the results and do not allow us to get quantitative information. Furthermore, there were quite many deliberate changes as well as errors

and other unintentional variation between the experiments. These makes comparison between the experiments even harder. The deliberate changes were caused both by changes in the scope of the thesis and improvements in the setup as I needed to learn by experimenting. Secondly, the time between ending of the reaction and characterization was sometimes quite long. Even with the washing and storing of the product in MQ water in nitrogen atmosphere, the particles probably experienced at least some morphological changes of some degree. It would be better to analyze the particles almost straight after the reaction. Additionally, taking samples of the particles during the reaction could provide information on the growth mechanism of the particles. Now, it was impossible to tell if the morphology and particle size seen in the electron microscope images resulted from some stage of the reaction or changes during the storage. Thirdly, the effects of NaOH could studied much more thoroughly with an improved experiment series in order to get more accurate and precise information. The experiments should be done at a higher temperature, e.g., at 50 ˚C, changing only the initial NaOH concentration. It might also be useful to measure the pH level constantly, and more accurately than was possible in this work, during reaction or keep the pH level constant by adding NaOH as it is consumed in the reaction. Lastly, the laboratory scale limits the applicability of the results for the hard metal and other industries. The growth of the particles might be more even and the distribution of the particle size narrower were the reaction batches larger. On the other hand, the laboratory-scale experiments are suitable for gaining basic understanding of the reaction and crucial for planning larger-scale experiments.

My suggestions for future research include dispersion stabilization experiments as well as experiments focusing on conversion rate and yield. The dispersion stabilization experiments could be performed using both nano- and micron-scale Co particles. The particle size and the size and type of surfactant required are probably related, as smaller particles are easier to disperse evenly. The particle size could be determined

using the dynamic light scattering technique (DLS). The stability of the dispersion could be estimated measuring the zeta potential of the double layer with the electrophoretic light scattering technique (ELS). On the other hand, one could use a centrifuge for quick testing before longer sedimentation tests with selected surfactants. There could be a surfactant for dispersing the particles after the end of the reaction and another in-situ surfactant for modifying the particle growth and inhibiting agglomeration in the first place. The conversion rate experiments could be based on the Phase2 experiments. The reaction temperatures could be, for example, 50, 55, and 60 ˚C, as at 65 ˚C the reaction could not be controlled in the thesis. The pH level would preferably be maintained constant by monitoring and adding more NaOH as the reaction progresses. Samples of the reaction solution should be taken before, during and after the reaction. These samples could be analyzed for the cobalt ion concentrations using the atomic absorption spectrometry technique (AAS). Both stability of the dispersion and the conversion rate are essential for developing a viable and economic method to produce and preserve cobalt particles to be used in the hard metal production.

References

[1] Yang, H, Shen, C, Song, N, Wang, Y, Yang, T, Gao, H & Cheng, Z, "Facile synthesis of hollow nano-spheres and hemispheres of cobalt by polyol reduction," *Nanotechnology,* 2010, 21, 375602, 5 pp.

[2] Medvedeva, OI, Kambulova, SS, Bondar, OV, Gataulina, AR, Ulakhovich, NA, Gerasimov, AV, Evtugyn, VG, Gilmutdinov, IF & Kutyreva, MP, "Magnetic Cobalt and Cobalt Oxide Nanoparticles in Hyperbranched Polyester Polyol Matrix," *J Nanotechnology,* 2017, 7607658, 9 pp.

[3] Joseyphus, RJ, Matsumoto, T, Takahashi, H, Kodama, D, Tohji, K & Jeyadevan, B, "Designed synthesis of cobalt and its alloys by polyol process," *J Solid State Chem,* 2007, 180:11, 3008-3018.

[4] Cao, G, "Nanostructures and Nanomaterials: Synthesis, Properties and Applications," 2nd Ed, UK: Imperial College Press, 2004, 1-448.

[5] Neikov, OD, "Introduction," In Handbook of Non-Ferrous Metal Powders, Edited Neikov, OD, Naboychenko, SS & Dowson, G, 1st Ed, Great Britain: Elsevier Ltd, 2009, 1-4.

[6] Tong, Y, Dong, X & Qi, M, "High performance magnetorheological fluids with flower-like cobalt particles," *Smart Mater and Struct,* 26:2, 2017, 1-7.

[7] Chen, H, Liu, Y & Zhao, G, "Controlled synthesis and characterisation of flower-like cobalt microstructures," *Micro Nano Lett,* 6:3, 2011, 122-124.

[8] Abdelkareem, MA, Sayed, ET, Alawadhi, H, & Alami, AH, "Synthesis and testing of cobalt leaf-like nanomaterials as an active catalyst for ethanol oxidation," *Int J Hydrogen Energy,* 45:35, 2020, 17311-17319.

[9] Salman, SA, Usami, T, Kuroda, K & Okido, M, "Synthesis and Characterization of Cobalt Nanoparticles Using Hydrazine and Citric Acid," *J. Nanotechnol.,* 14, 2014, 1-6.

[10] Li, Y, Zhao, J, Zhu, Y, Ma, D, Zhao, Y, Hou, S, Yan, F & Wang, Z, "Controlled synthesis of rice ear-like cobalt microcrystals at room temperature," *Colloid Surface A,* 356:1-3, 2010, 156-161.

[11] Liu, X, Yi, R, Wang, Y, Qiu, G, Zhang, N & Li, X, "Highly Ordered Snowflakelike Metallic Cobalt Microcrystals," *J Phys Chem C,* 111:1, 2007, 163-167.

[12] Upadhyaya, GS, "2.0 Production of Cobalt Powder," In Cemented tungsten carbides : production, properties, and testing, Westwood, N.J.: Noyes Publications, 1998, 72-74.

[13] Pastor, H, Bonneau, M & Pillot J, "New spherical monodisperse and non-agglomerated cobalt powder," *International Conference on Advances in Hard Materials Production,* Bonn, Germany, Paper No 6; EPMA, Shrewsbury, UK, 1992.

[14] LaMer, VK & Dinegar, RH , "Theory, Production and Mechanism of Formation of Monodispersed Hydrosols," *J. Am. Chem. Soc.,* 1950, 72:11, 4847–4854.

[15] Whitehead, CB, Özkar, S & Finke, RG, "LaMer's 1950 model of particle formation: a review and critical analysis of its classical nucleation and fluctuation theory basis, of competing models and mechanisms for phase-changes and particle formation, and then of its application to silver halide...," *Materials Advances,* 2021, 75 pp.

[16] Balela, MD, "Synthesis and Characterization of Cobalt Nanoparticles Prepared by Liquid-phase Reduction," Master's Thesis, Universiti Sains Malaysia, 2008, 1-168.

[17] Viau, G, Fiévet-Vincent, F & Fiévet, F, "Nucleation and growth of bimetallic CoNi and FeNi monodisperse particles prepared in polyols," *Solid State Ionics,* 84, 1996, 259-270.

[18] Fievet, F, Lagier, JP & Figlarz, M, "Preparing Monodisperse Metal Powders in Micrometer and Submicrometer Sizes by the Polyol Process," *MRS Bull.,* 14:12, 1989, 29-34.

[19] Djokić, SS, "Electroless Deposition of Cobalt Using Hydrazine as a Reducing Agent," *J. Electrochem. Soc.,* 144:7, 1997, 2358-2363.

[20] Nichols, G, Byard, S, Bloxham, MJ, Botterill, J, Dawson, NJ, Dennis, A, Diart, V, North, N & Sherwood, JD, "A review of the terms agglomerate and aggregate with a recommendation for nomenclature used in powder and particle characterization," *J. Pharm. Sci.,* 91, 2002, P2103-2109.

[21] Nützenadel, C, Züttel, A, Chartouni, D, Schmid, G & Schlapbach, L, "Critical size and surface effect of the hydrogen interaction of palladium clusters," *Eur. Phys. J. D,* 8:2, 2000, 245-250.

[22] Yu, S, Sun, C-J & Chow, G-M, "Chemical Synthesis of Nanostructured Particles and Films," In Nanostructured Materials - Processing, Properties, and Applications, Edited Koch CC, 2nd Ed, William Andrew Publishing, 2007, 3-46.

[23] T. Tadros, "General Introduction," In Dispersion of Powders in Liquids and Stabilization of Suspensions, Weinheim, Germany: Wiley-VCH, 2012, 1-16.

[24] Boinovich L, "LVO forces in thin liquid films beyond the conventional DLVO theory," *Current Opinion in Colloid & Interface Science,* 15:5, 2010, 297-302.

[25] Hotze EM, Phenrat T & Lowry GV, "Nanoparticle aggregation: challenges to understanding transport and reactivity in the environment," *J Environ Qual,* 39:6, 2010, 1909-1924.

[26] Andrade, ÂL, Fabris, JD, Ardisson, JD, Valente, MA & Ferreira, JMF, "Effect of Tetramethylammonium Hydroxide on Nucleation, Surface Modification and Growth of Magnetic Nanoparticles," *J. Nanomater.,* Vol. 2012, 2012, 10.

[27] Department of Physics, The Chinese University of Hong Kong, "Atomic World, Basic principle of transmission electron microscope," *The Government of the Hong Kong Special Administrative Region of the People's Republic of China – Education Bureau,* (http://www.hk-phy.org/atomic_world/tem/tem02_e.html; accessed 18.06.2018).

[28] Havancsák, K, "High-Resolution Scanning Electron Microscopy," Department of Materials Physics, Eötvös Loránd University, (https://www.technoorg.hu/news-and-events/articles/high-resolution-scanning-electron-microscopy-1/; accessed 29.05.2022).

[29] Wyckoff, RWG, "Hexagonal closest packed, hcp, structure," In Crystal Structures - Volume 1, 2. Ed., New York: Interscience Publishers, 1963, 7-83..

[30] Williams GI & Owen EA, "A low-temperature X-ray camera," *J. Sci. Instrum.,* 31, 1954, 49-54.

[31] Lotmar W & Feitknecht W, "Über Änderungen der Ionenabstände in Hydroxyd - Schichtengittern," *Z. Kristallogr. Krist.,* 93, 1936, 368-378.

[32] Shafi, KVPM, Gedanken, A & Pozorov, R, "Surfactant-Assisted Self-Organization of Cobalt Nanoparticles in a Magnetic Fluid," *Adv. Mater.,* 10:8, 1998, 590-593.

[33] López- López, MT, Kuzhir, P & Meunier, A & Bossis, G, "Synthesis and magnetorheology of suspensions pf submicron-sized cobalt particles with tunable particle size," *J. Phys.: Condens. Matter,* 22:32, 2010, 324106 (6 pp).

[34] Alex, P, Majumdar, S, Kishor, J & Sharma IG, "Synthesis of Cobalt Nano Crystals in Aqueous Media and Its Characterization," *MSA,* 2:9, 2011, 1307-1312.

[35] Kalyan Kamal, SS, Sahoo, PK, Premkumar, M, Rama Rao, NV, Jagadeesh Kumar, T, Sreedhar, B, Singh, AK, Ram, S & Chandra Sekhar, K, "Synthesis of cobalt nanoparticles by a modified polyol process," *J. Alloys Compd.,* 474:1-2, 2009, 214-218.

[36] An, S-H, Kim, S-H, Lee, J-H, Hong, H-S & Kim, Y-D, "Synthesis of Nano Sized Cobalt Powder from Cobalt Sulfate Heptahydrate by Liquid Phase Reduction," *Kor. J. Mater. Res.,* 21:6, 2011, 327-333.

[37] Babick, F, "Suspensions of Colloidal Particles and Aggregates," 2nd ed, Cham : Springer International Publishing AG, 2016, 341.

[38] Naboychenko, SS, Murashova, IB & Neikov, OD, "Production of Cobalt and Cobalt-Alloy Powders," In Handbook of Non-Ferrous Metal Powders, Edited Neikov, OD, Naboychenko, SS & Dowson, G, 1st Ed, Great Britain: Elsevier Ltd, 2009, 399-408.